cmgh
CELLULAR AND MOLECULAR GASTROENTEROLOGY AND HEPATOLOGY

ORIGINAL RESEARCH

Prolonged Administration of Melatonin Ameliorates Liver Phenotypes in Cholestatic Murine Model

Ludovica Ceci,[1,2] Lixian Chen,[1] Leonardo Baiocchi,[3] Nan Wu,[1] Lindsey Kennedy,[1,4] Guido Carpino,[5] Konstantina Kyritsi,[1] Tianhao Zhou,[1] Travis Owen,[1] Debjyoti Kundu,[1] Amelia Sybenga,[6] Abdulkadir Isidan,[7] Burcin Ekser,[7] Antonio Franchitto,[2] Paolo Onori,[2] Eugenio Gaudio,[2] Romina Mancinelli,[2] Heather Francis,[1,4] Gianfranco Alpini,[1,4,§] and Shannon Glaser[8,§]

[1]Division of Gastroenterology and Hepatology, Department of Medicine, Indiana University School of Medicine, Indianapolis, Indiana; [2]Department of Anatomical, Histological, Forensic Medicine and Orthopedics Sciences, Sapienza University of Rome, Rome, Italy; [3]Unit of Hepatology, Tor Vergata University, Rome, Italy; [4]Department of Research, Richard L. Roudebush VA Medical Center, Indianapolis, Indiana; [5]Department of Movement, Human and Health Sciences, University of Rome "Foro Italico," Rome, Italy; [6]Department of Pathology and Laboratory Medicine, University of Vermont Medical Center, Burlington, Vermont; [7]Division of Transplant Surgery, Department of Surgery, Indiana University School of Medicine, Indianapolis, Indiana; and [8]Department of Medical Physiology, Texas A&M University, Bryan, Texas

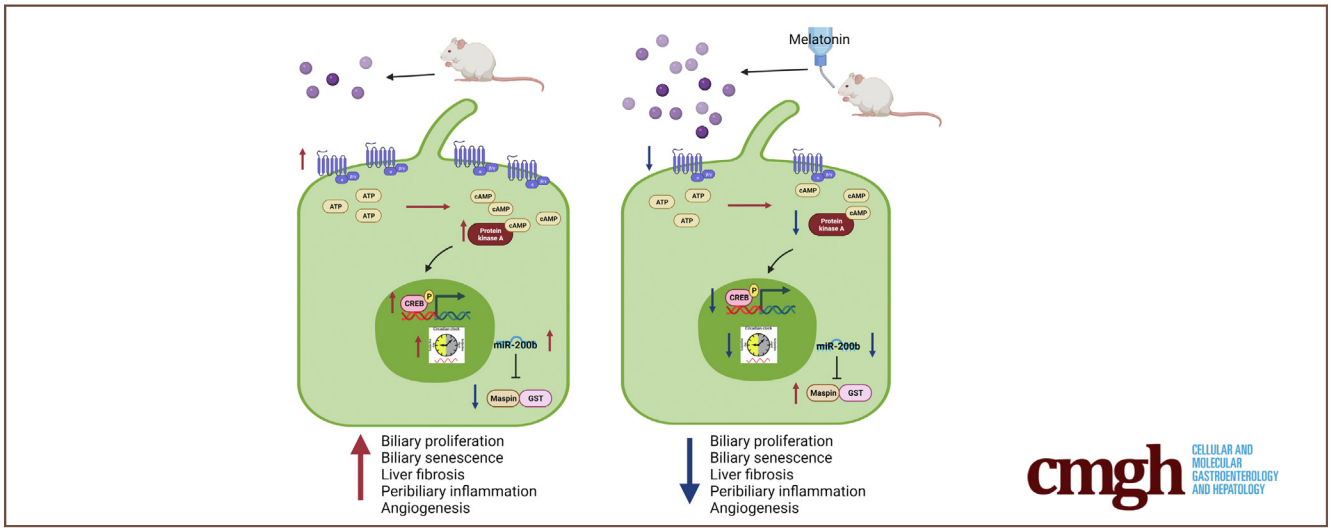

SUMMARY

Prolonged administration of melatonin (1.03 mg intake per mouse per day) in *Mdr2*$^{-/-}$ mice improves liver histology and restores the circadian rhythm by interaction with Melatonin receptor 1 (MT1) through decreased angiogenesis and increased glutathione-S transferase activity. Manipulation of clock genes/*miR200b* pathway by melatonin treatment may be a therapeutic option for primary sclerosing cholangitis patients.

BACKGROUND & AIMS: Primary sclerosing cholangitis (PSC) is characterized by biliary senescence and hepatic fibrosis. Melatonin exerts its effects by interacting with Melatonin receptor 1 and 2 (MT1/MT2) melatonin receptors. Short-term (1 wk) melatonin treatment reduces a ductular reaction and liver fibrosis in bile duct–ligated rats by down-regulation of MT1 and clock genes, and in multidrug resistance gene 2 **knockout** (*Mdr2*$^{-/-}$) mice by decreased *miR200b*-dependent angiogenesis. We aimed to evaluate the long-term effects of melatonin on liver phenotype that may be mediated by changes in MT1/clock genes/*miR200b*/maspin/glutathione-S transferase (GST) signaling.

METHODS: Male wild-type and *Mdr2*$^{-/-}$ mice had access to drinking water with/without melatonin for 3 months. Liver damage, biliary proliferation/senescence, liver fibrosis, peribiliary inflammation, and angiogenesis were measured by staining in liver sections, and by quantitative polymerase chain reaction and enzyme-linked immunosorbent assay in liver samples. We confirmed a link between MT1/clock genes/*miR200b*/maspin/GST/angiogenesis signaling by Ingenuity

Pathway Analysis software and measured liver phenotypes and the aforementioned signaling pathway in liver samples from the mouse groups, healthy controls, and PSC patients and immortalized human PSC cholangiocytes.

RESULTS: Chronic administration of melatonin to *Mdr2*$^{-/-}$ mice ameliorates liver phenotypes, which were associated with decreased MT1 and clock gene expression.

CONCLUSIONS: Melatonin improves liver histology and restores the circadian rhythm by interaction with MT1 through decreased angiogenesis and increased maspin/GST activity. *(Cell Mol Gastroenterol Hepatol 2022;14:877–904; https://doi.org/10.1016/j.jcmgh.2022.07.007)*

Keywords: Cholangiopathies; Ductular Reaction; Circadian Rhythm; TGFβ1.

Primary sclerosing cholangitis (PSC) is a cholestatic liver disease (incidence, <1/100,000) leading to biliary strictures, recurrent cholangitis, and biliary cancer.[1] Reliable drug therapy still is lacking, thus prompting studies on the molecular mechanisms regulating PSC progression are needed. The multidrug resistance protein 2 (*Mdr2*$^{-/-}$) mouse model resembles some features of human PSC such as concentric periductal fibrosis with onion-skin shape, suggesting the appropriateness of this model.[2] The phenotypes of PSC are evidenced by increased ductular reaction (DR) and biliary senescence that causes the release of senescence-associated secretory phenotypes, thus contributing to the paracrine activation of hepatic stellate cells (HSCs) and collagen deposition.[3–5] There is increasing information in mouse models and human samples regarding the role of gastrointestinal hormones and neurotransmitters (eg, secretin and melatonin) in the modulation of PSC phenotypes.[5,6] Melatonin, which regulates and is regulated by the circadian rhythm in mammals through interaction with MT1 and MT2 melatonin receptors, is synthesized from serotonin by the pineal gland and the biliary epithelium by the enzyme aralkyl amine N-acetyltransferase (AANAT).[7,8] Several studies have identified the role of melatonin in the regulation of cholestatic liver diseases.[5,8–14] For example, melatonin protects cholangiocytes from oxidative stress–induced inflammation by inhibiting nuclear factor-κB signaling.[11] In addition, melatonin ameliorates liver damage in several cholestatic liver diseases, in both early and advanced stages, and nonalcoholic fatty liver diseases.[9] We have shown that short-term (1 wk) administration of melatonin or exposure to complete dark (which increases melatonin levels), modulation of AANAT, pinealectomy (which decreases melatonin synthesis), or down-regulation of MT1 (by which melatonin exerts its effects) modulates DR, biliary senescence, liver angiogenesis, and fibrosis by a paracrine pathway through changes in biliary transforming growth factor β1 (TGFβ1)/transforming growth factor β1 receptor signaling.[5,8,12–14] Cholestatic bile duct–ligated (BDL) rats treated with melatonin for 1 week have decreased biliary hyperplasia through MT1 interaction that down-regulates 3′-5′-cyclic adenosine monophosphate (cAMP)-dependent protein kinase A (PKA) phosphorylation and the expression of selected clock genes.[8] Furthermore, treatment of *Mdr2*$^{-/-}$ mice with melatonin or dark therapy (which increases melatonin synthesis) reduces cholestatic phenotypes such as DR, biliary senescence, and liver fibrosis through down-regulation of *miR200b*-dependent angiogenesis, which regulates biliary damage and liver fibrosis in cholestatic liver diseases including PSC.[5,6,15–17] Overexpression of AANAT (which increases melatonin levels) reduces DR, biliary damage, and liver fibrosis.[5,13] Conversely, in BDL rats subjected to pinealectomy (which reduces AANAT expression and melatonin levels) there was enhanced biliary senescence and liver fibrosis through enhanced expression of clock genes and *miR200b*.[13] Melatonin ameliorates cholestatic phenotypes through down-regulation of MT1, which reduces biliary damage and liver fibrosis by down-regulation of cAMP/G protein-coupled receptor 50 (GPR50)/TGFβ1/TGFβ1 receptor signaling. In contrast, the knockout of MT2 worsens biliary and liver damage by activating this transduction pathway.[14] Exploring the short-term modulation of melatonin signaling is a shortcoming of our previous studies[5,13,14]; thus, we aimed to perform experiments to evaluate the long-term treatment of melatonin administration on PSC phenotypes and the associated downstream signaling mechanisms.

Results

Measurement of Immunoreactivity/Expression of AANAT, and Melatonin Levels in Serum

Parallel to previous studies,[5,13] we showed immunoreactivity of AANAT in both mouse and human bile ducts (Figure 1*B*). There was weak immunoreactivity of AANAT in hepatocytes from *Mdr2*$^{-/-}$ mice, but no immunoreactivity for AANAT was seen in HSCs (Figure 2, white arrows). Biliary immunoreactivity and messenger RNA (mRNA) expression of *Aanat* were higher (owing to a compensatory mechanism)

§Authors share co-senior authorship.

Abbreviations used in this paper: **AANAT, aralkyl amine N-acetyltransferase; ARNTL, Arnt-like protein-1; BDL, bile duct ligation; cAMP, 3′-5′-cyclic adenosine monophosphate; CD, cluster of differentiation; CK19, cytokeratin 19; Colla1, collagen, type I a; CREB, cAMP response element-binding protein; DR, ductular reaction; GST, glutathione S-transferase; HNF4α, hepatocyte nuclear factor 4α; HSC, hepatic stellate cell; IBDM, intrahepatic bile duct mass; IHC, immunohistochemistry; iNOS, inducible nitric oxide synthase; Mdr2, multidrug resistance protein 2; mRNA, messenger RNA; NPC, nonparenchymal cell; PCNA, proliferating cell nuclear antigen; pCREB, phospho-cAMP response element-binding protein; PKA, protein kinase A; pPKA, phospho-protein kinase A; PSC, primary sclerosing cholangitis; p16, cyclin-dependent kinase inhibitor 2A; qPCR, quantitative polymerase chain reaction; SA-β-GAL, senescence-associated β-galactosidase; TGFβ1, transforming growth factor-β1; VEGFA, vascular endothelial growth factor-A; WT, wild type.**

Most current article

2352-345X
https://doi.org/10.1016/j.jcmgh.2022.07.007

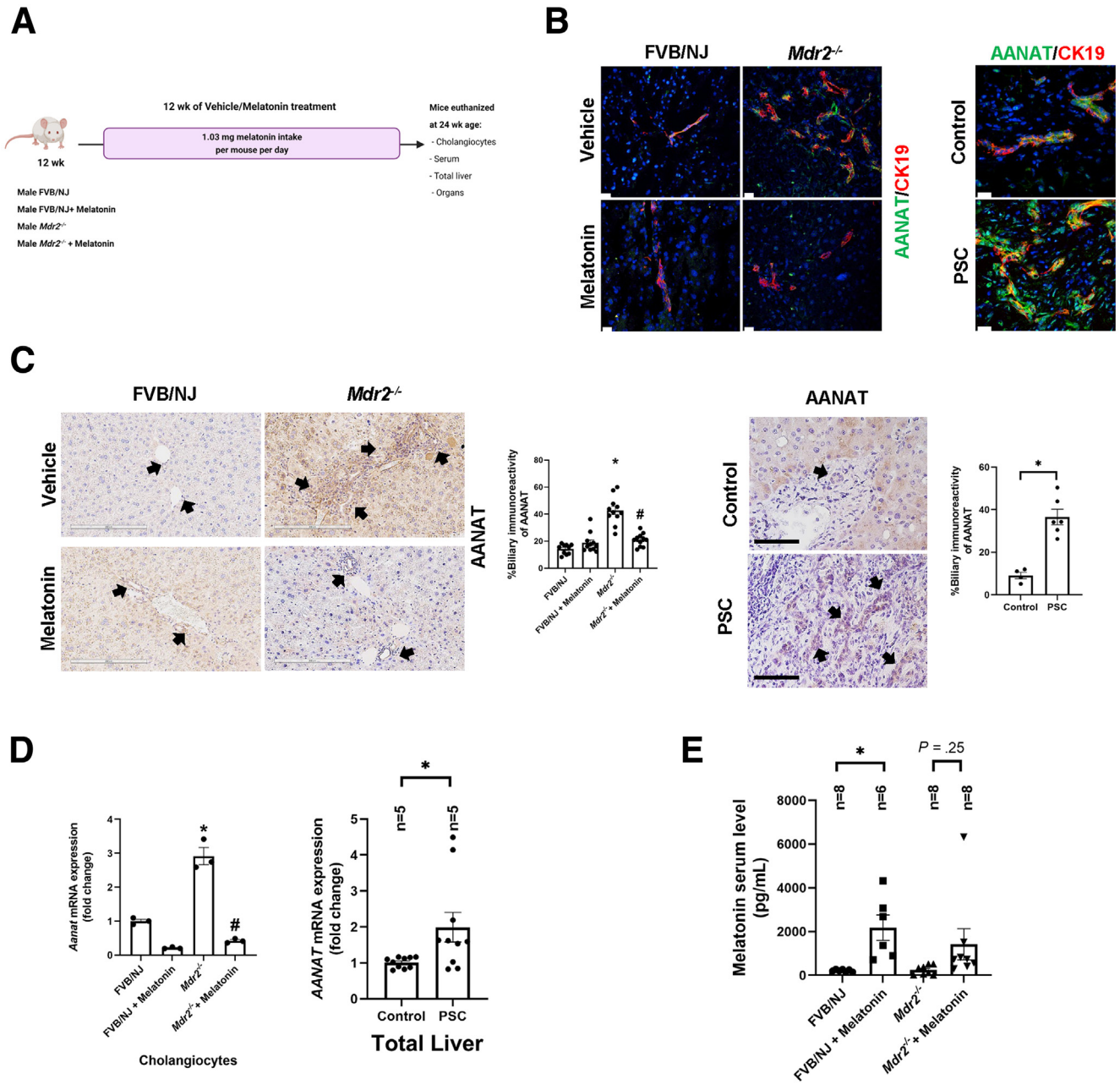

Figure 1. (*A*) Experimental design: both male FVB/NJ and *Mdr2*$^{-/-}$ mice at 12 weeks underwent vehicle/melatonin treatment for 12 weeks. Mice were killed at 24 weeks and we isolated cholangiocytes as well as collected liver, organs, and serum. The graphic for the experimental design was created with BioRender.com. (*B*) Using immunofluorescence for AANAT (green) in liver sections (co-stained with CK19, red) there is increased biliary immunoreactivity in both *Mdr2*$^{-/-}$ (*left*) and human PSC groups (*right*) compared with control groups, which is reduced after melatonin treatment. Original magnification, 20×; *scale bar*: 20 μm. (*C*) IHC of AANAT in both murine (original magnification, 20×; *scale bar*: 200 μm) and human PSC groups (n = 2 control, n = 3 PSC samples; original magnification, 20×; *scale bar*: 100 μm). Data are means ± SEM of 10 nonoverlapping random fields of 5 mice per group. *$P < .05$ vs WT; #$P < .05$ value vs *Mdr2*$^{-/-}$ mice. Data are means ± SEM of 4 normal and 6 PSC nonoverlapping random fields of n = 2 normal control and n = 3 PSC samples. $P < .05$ vs normal control. Each *dot* represents 1 value in data set. (*D*) mRNA expression of *Aanat* in both isolated cholangiocytes and total liver human samples (n = 5 control and n = 5 PSC) is increased in PSC groups, which is reduced after melatonin treatment. (*E*) Serum levels of melatonin was increased in both WT and *Mdr2*$^{-/-}$ mice after 12 weeks of melatonin treatment. Each *dot* represents 1 value in data set. Data are means ± SEM of 3 evaluations from 3 cumulative preparations of cholangiocytes from 6 mice per group. *$P < .05$ vs WT or control; #$P < .05$ vs Mdr2$^{-/-}$ mice.

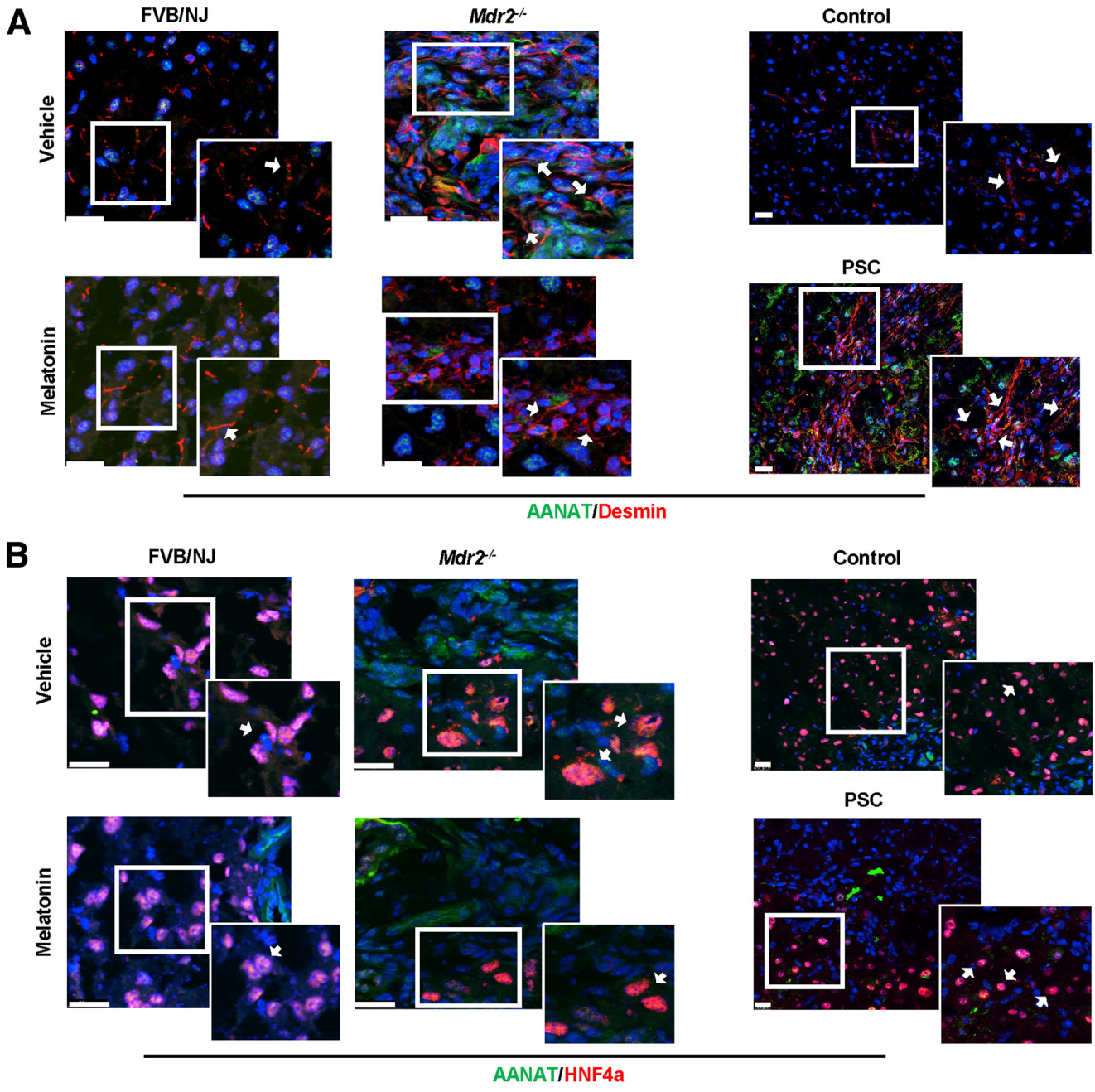

Figure 2. AANAT expression in hepatocytes and cholangiocytes. By immunofluorescence, (*A*) HSCs (red, desmin) showed no indication of AANAT (green) in both murine and PSC samples compared with their respective control group, and (*B*) low expression of AANAT in hepatocytes (red), which is reduced after melatonin treatment. Original magnification of the murine model, 100× (*left*), and the actual magnification of the human sample is 20× (*right*). *Scale bars*: 20 μm. The *white box* shows a high-magnification picture: 40× (human staining) and 50× (murine staining). *White arrows* in the *white box* indicate the expression of AANAT in both HSCs and hepatocytes.

in both 24-week-old *Mdr2*$^{-/-}$ mice (reduced after 12-week melatonin treatment) and late-stage human PSC samples (Figure 1*C* and *D*). Previously, we showed that the melatonin serum levels of *Mdr2*$^{-/-}$ at 12 weeks were increased significantly compared with the wild-type (WT) mice, likely owing to a compensatory mechanism.[5] However, in our current study, melatonin serum levels decreased in 24-week *Mdr2*$^{-/-}$ mice (mimicking late-stage PSC), but were higher in *Mdr2*$^{-/-}$ mice treated with melatonin (Figure 1*E*). The reduction of melatonin serum levels observed in 24-week *Mdr2*$^{-/-}$ mice is supported by a study showing that serum melatonin levels decrease with age and are reduced by 80% in 27-month-old mice compared with 12-month-old mice.[18] The reduced melatonin serum levels in 24-week-old *Mdr2*$^{-/-}$ mice (which had enhanced AANAT mRNA expression) likely are owing to increased post-transcriptional degradation of melatonin.

Table 1. Assessment of Liver Weight, Body Weight, and Liver to Body Weight Ratio

Group	BW, *g*	LW, *g*	LW/BW ratio, %
FVB/NJ (n = 10)	32.4 ± 0.5	1.6 ± 0.1	4.88 ± 0.37
FVB/NJ + melatonin (n = 8)	34.1 ± 0.7	2.0 ± 0.1	5.82 ± 0.29
Mdr2$^{-/-}$ (n = 10)	33.3 ± 0.5	2.5 ± 0.06[a]	7.6 ± 0.2[a]
Mdr2$^{-/-}$ + melatonin (n = 9)	35.6 ± 0.9	2.6 ± 0.09	7.3 ± 0.1

BW, body weight; LW, liver weight.
[a]$P < .05$ vs FVB/NJ.

Chronic Administration of Melatonin Reduces Liver Damage and Intrahepatic Bile Duct Mass

The liver to body weight ratio (index of liver cell growth)[19] was higher in *Mdr2*$^{-/-}$ compared with WT mice; there was no significant difference in liver to body weight ratio between *Mdr2*$^{-/-}$ mice compared with *Mdr2*$^{-/-}$ mice treated with melatonin (Table 1). Twenty-four–week-old *Mdr2*$^{-/-}$ (n = 9) mice showed increased portal fibrosis with few bridges and a mild to focally moderate increase in bile duct mass and DR (supported by cytokeratin 19 [CK19] immunohistochemistry [IHC]) (Figure 3*C*). We observed mild patchy portal inflammation, prominent diffuse bile stasis, and variable reactive changes in hepatocytes with rare acidophil bodies. *Mdr2*$^{-/-}$ mice treated with melatonin (n = 8) showed periportal fibrosis, portal tracts expanded by moderate chronic inflammatory infiltrate with mild interface activity, and diffuse DR. Furthermore, we observed variable reactive changes in hepatocytes with rare acidophil bodies and atrophic epithelium in the periportal zone with minimal inflammation; no significant pathologic changes were observed in the other organs among the experimental groups (Figure 4). The number of proliferating cellular nuclear antigen (PCNA)-positive cholangiocytes (also confirmed by quantitative polymerase chain reaction (qPCR) for *Pcna* in isolated cholangiocytes (Figure 3*B*) and intrahepatic bile duct mass (IBDM) increased markedly in 24-week *Mdr2*$^{-/-}$ mice compared with WT mice, which was reduced significantly in *Mdr2*$^{-/-}$ mice treated with melatonin; no changes in the number of PCNA-positive cholangiocytes and IBDM were observed between WT animals treated with melatonin compared with WT control mice (Figure 3*A*–*C*).

Long-Term Treatment With Melatonin Ameliorates Biliary Senescence in Mdr2$^{-/-}$ *Mice*

By staining for both senescence-associated β-galactosidase (SA-β-GAL) and cyclin-dependent kinase inhibitor 2A (p16) in liver sections, as well as qPCR for p16 (*Cdkn2a*) and cyclin-dependent kinase inhibitor 1A (*Cdkn1a*) in isolated cholangiocytes, there was enhanced biliary senescence in *Mdr2*$^{-/-}$ compared with WT mice, which was decreased in *Mdr2*$^{-/-}$ mice treated with melatonin compared with the corresponding *Mdr2*$^{-/-}$ mice. No changes in biliary senescence were observed between WT animals treated with melatonin compared with WT control mice (Figure 5).

Liver Fibrosis Is Reduced in Mdr2$^{-/-}$ *Mice Treated With Melatonin for 12 Weeks*

By Fast Green/Sirius Red and Masson Trichrome staining, collagen deposition was higher in *Mdr2*$^{-/-}$ compared with WT mice, an increase that was reduced in *Mdr2*$^{-/-}$ mice treated with melatonin compared with the corresponding *Mdr2*$^{-/-}$ mice. No changes in collagen deposition were observed between WT animals treated with melatonin compared with WT control mice (Figure 6*A* and *B*). There was enhanced mRNA expression of collagen, type I a (*Col1a1*) and *Tgfb1* in the total liver, as well as TGFβ1 level in cholangiocyte supernatant from *Mdr2*$^{-/-}$ compared with WT mice, which was decreased in *Mdr2*$^{-/-}$ mice treated with melatonin. No changes in these phenotypes were observed between WT animals treated with melatonin compared with WT control mice (Figure 6*C* and *D*).

Prolonged Melatonin Administration Alleviates Portal Inflammation in Mdr2$^{-/-}$ *Mice*

Several studies have shown the role of hepatic macrophages in PSC progression[20] and how melatonin reduces inflammation by promoting antioxidant events.[11] With this background, we measured the effect of chronic melatonin treatment on liver inflammation and observed the following: (1) human PSC (n = 3) samples have increased cluster of differentiation 80 (CD80)-positive and CD206-positive macrophages compared with control groups (n = 2) (Figure 7*A*), as well as inducible nitric oxide synthase (iNOS)-positive cells (Figure 8*A*); (2) an increased number of F4/80-positive, interferon-regulatory factor 5–positive macrophages (Figure 5*B*) and iNOS-positive cells (Figure 8*C*) in *Mdr2*$^{-/-}$ mice compared with WT mice, which are reduced after melatonin treatment; (3) cholangiocytes from human PSC and *Mdr2*$^{-/-}$ mice expressed iNOS, which is involved in the generation of the free radical NO (proinflammatory mediator)[21]; (4) an increased number of CD206-positive macrophages in *Mdr2*$^{-/-}$ mice that was enhanced in *Mdr2*$^{-/-}$ mice treated with melatonin[22] (Figure 7*B*, middle panel); and (5) an increased mRNA expression of *Il1b* and *Il6* in total liver samples of *Mdr2*$^{-/-}$ compared with WT mice. These changes were reversed in *Mdr2*$^{-/-}$ mice treated with melatonin compared with *Mdr2*$^{-/-}$ mice (Figure 5*C*); no changes in liver inflammation were observed between WT animals treated with melatonin compared with WT control mice (Figures 7 and 8).

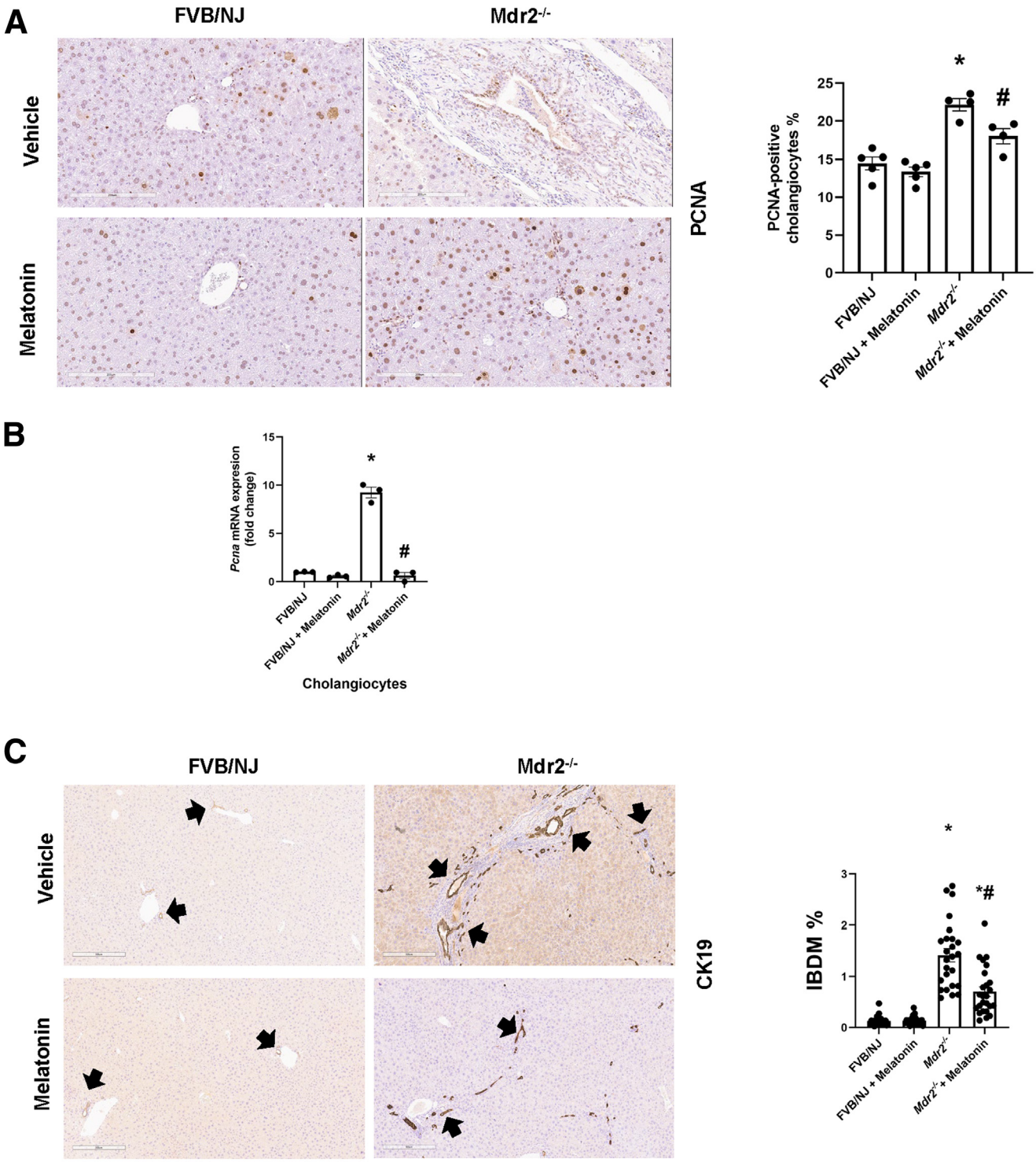

Figure 3. Biliary proliferation is reduced in *Mdr2*$^{-/-}$ mice treated with melatonin for 12 weeks. In *Mdr2*$^{-/-}$ mice, there was a significant increase in both (*A*) PCNA cholangiocyte–positivity (original magnification, 20×; *scale bar*: 200 μm; data are means ± SEM of 5 evaluations from n = 3 different animals per groups); (*B*) mRNA expression of *Pcna* in isolated cholangiocytes (data are means ± SEM of 3 evaluations from 3 cumulative preparations of cholangiocytes from 6 mice per group), as well as (*C*) IBDM compared with the WT group, which was reduced after melatonin treatment. Original magnification, 10×; *scale bar*: 300 μm. Data are means ± SEM of 24 nonoverlapping random fields of 5 mice per group. *Black arrows* indicate bile ducts. Each *dot* represents 1 value in data set. *$P < .05$ vs WT; #$P < .05$ vs *Mdr2*$^{-/-}$ mice.

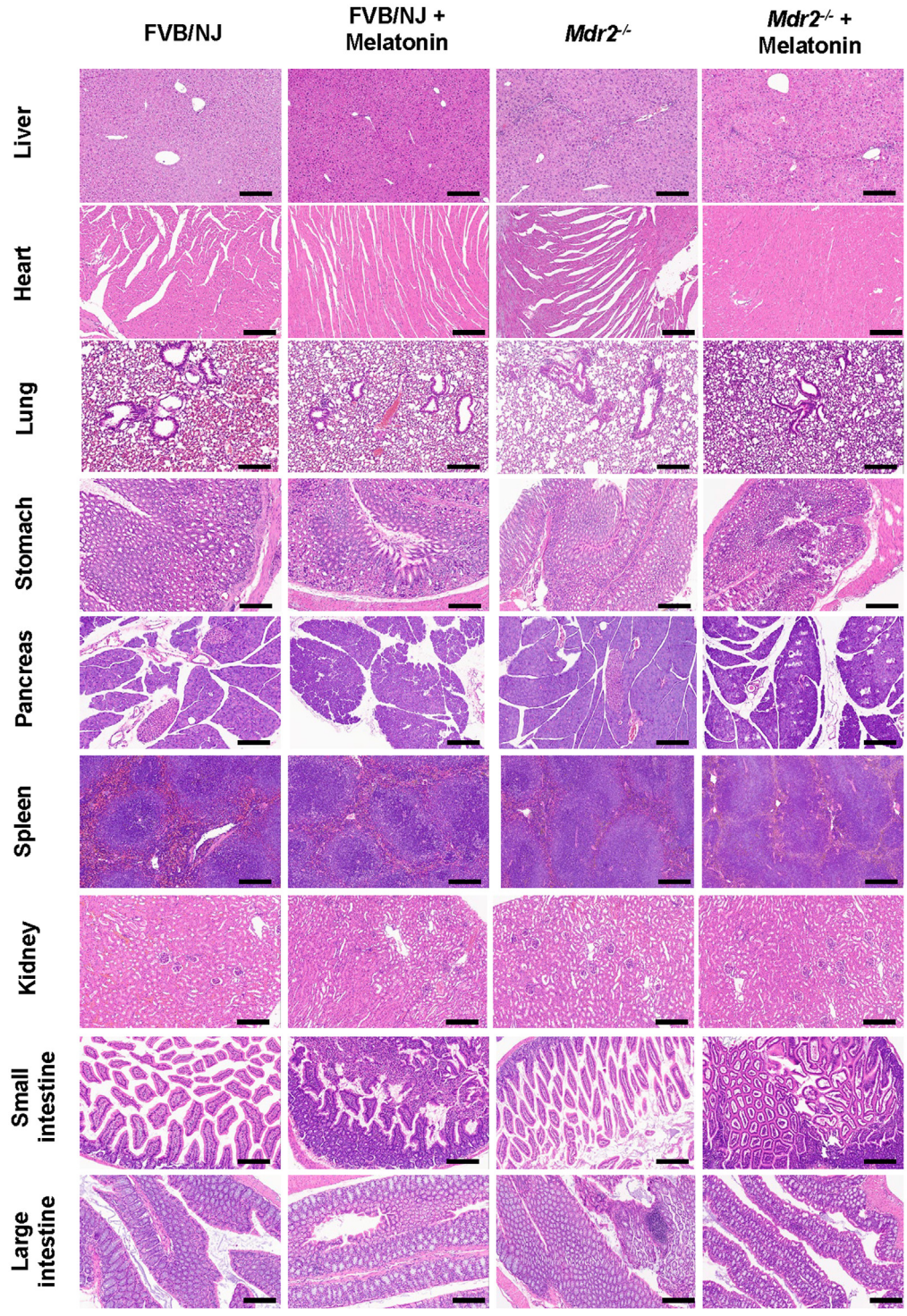

Figure 4. Melatonin ameliorates liver damage in *Mdr2*$^{-/-}$ mice. H&E staining of melatonin-treated *Mdr2*$^{-/-}$ mice showed mild to moderate portal inflammation with extension into and atrophy of bile duct epithelium, and atrophic epithelium in portal areas with minimal inflammation may suggest a biliary repair. No histomorphologic changes were observed among the organs of the experimental groups. Data are analyzed from n = 9-8 animals per each experimental group. Original magnification, 20×; *scale bars*: 200 μm.

Melatonin Reduces Angiogenesis in Mdr2$^{-/-}$ *Mice*

Because several studies have shown that melatonin effects on hyperplastic and neoplastic liver phenotypes are mediated by decreased angiogenesis,[5,13,23] and because vascular endothelial growth factor A (VEGFA) stimulates biliary proliferation,[24] we measured liver angiogenesis and VEGFA levels in our experimental setting. *Mdr2*$^{-/-}$ mice showed the following was enhanced:

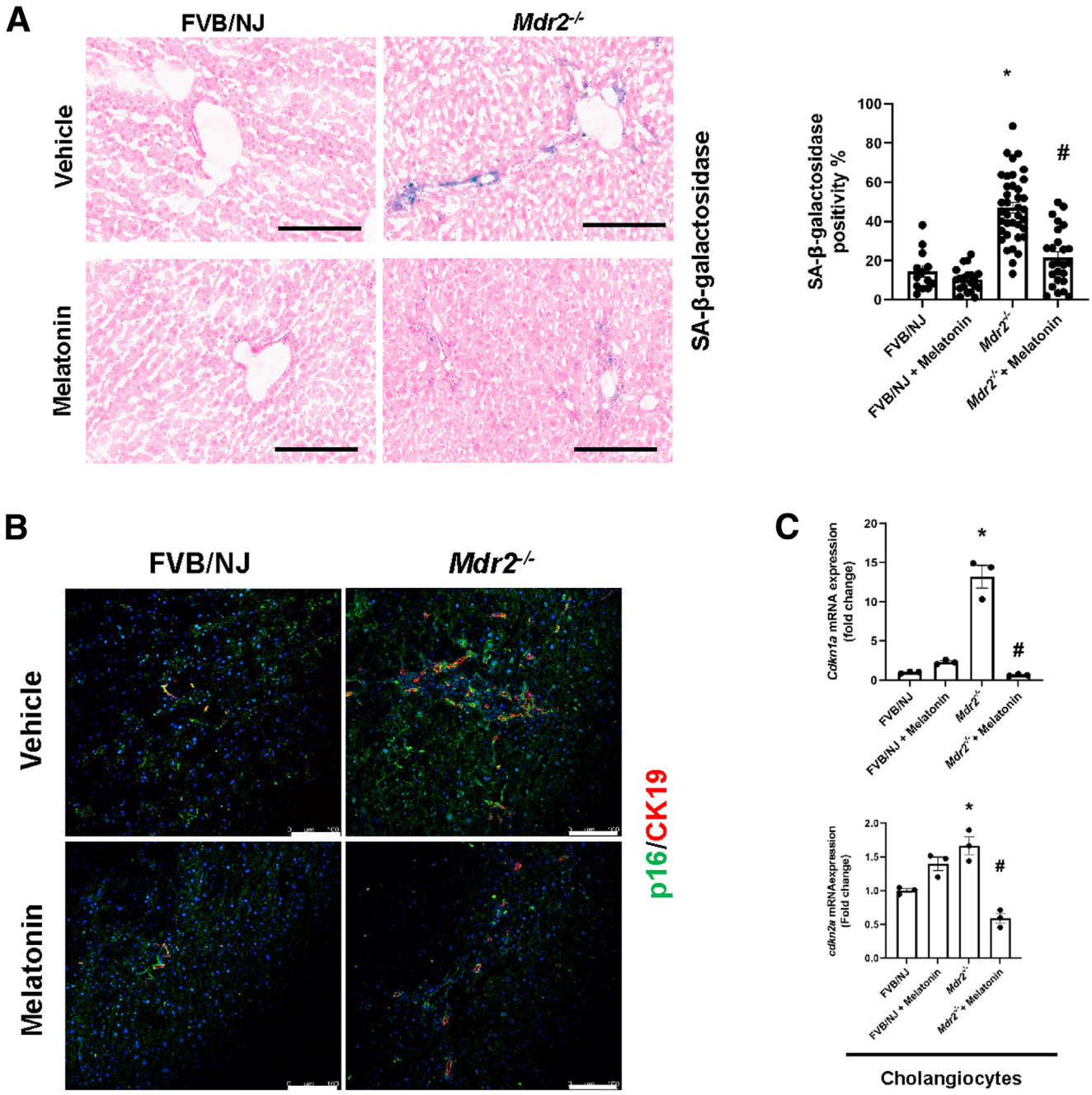

Figure 5. Melatonin prevents cholangiocyte senescence in Mdr2$^{-/-}$ mice. (*A*) By SA-β-GAL staining, *Mdr2*$^{-/-}$ mice have increased biliary senescence (blue) compared with WT, which is reduced in *Mdr2*$^{-/-}$ mice treated with melatonin for 12 weeks. Original magnification, 20×; *scale bars*: 200 μm. Data are means ± SEM of 20 pictures from n = 3 different animals per group. *<*P* vs WT; #<*P* vs *Mdr2*$^{-/-}$ mice. (*B*) Immunofluorescence staining for p16 (green) co-stained for CK19 (red) have increased immunoreactivity in *Mdr2*$^{-/-}$ mice, which is reduced after melatonin treatment for 12 weeks. Original magnification, 20×; *scale bars*: 100 μm. (*C*) *Cdnk2a* and *Cdnk1a* mRNA expression from isolated cholangiocytes of 12-week melatonin-treated Mdr2$^{-/-}$ mice were decreased when compared with *Mdr2*$^{-/-}$ mice. Each *dot* represents 1 value in data set. Data are means ± SEM of 3 evaluations from 3 cumulative preparations of cholangiocytes from 6 mice per group.

(1) immunoreactivity of VEGFA and CD31 in liver sections (Figure 9*A* and *B*); (2) mRNA expression of vascular endothelial growth factor C (*Vegfc*) and *Pecam1* (gene for CD31) in the total liver (Figure 9*C*); (3) mRNA expression of *Vegfa, Kdr* (gene for vascular endothelial growth factor receptor 2) and for *Flt4* (gene for vascular endothelial growth factor receptor 3) in cholangiocytes (Figure 9*D*); and (4) VEGFA levels in cholangiocyte supernatant (Figure 6*E*); these phenotypes were reduced in *Mdr2*$^{-/-}$ mice treated with melatonin (Figure 9).

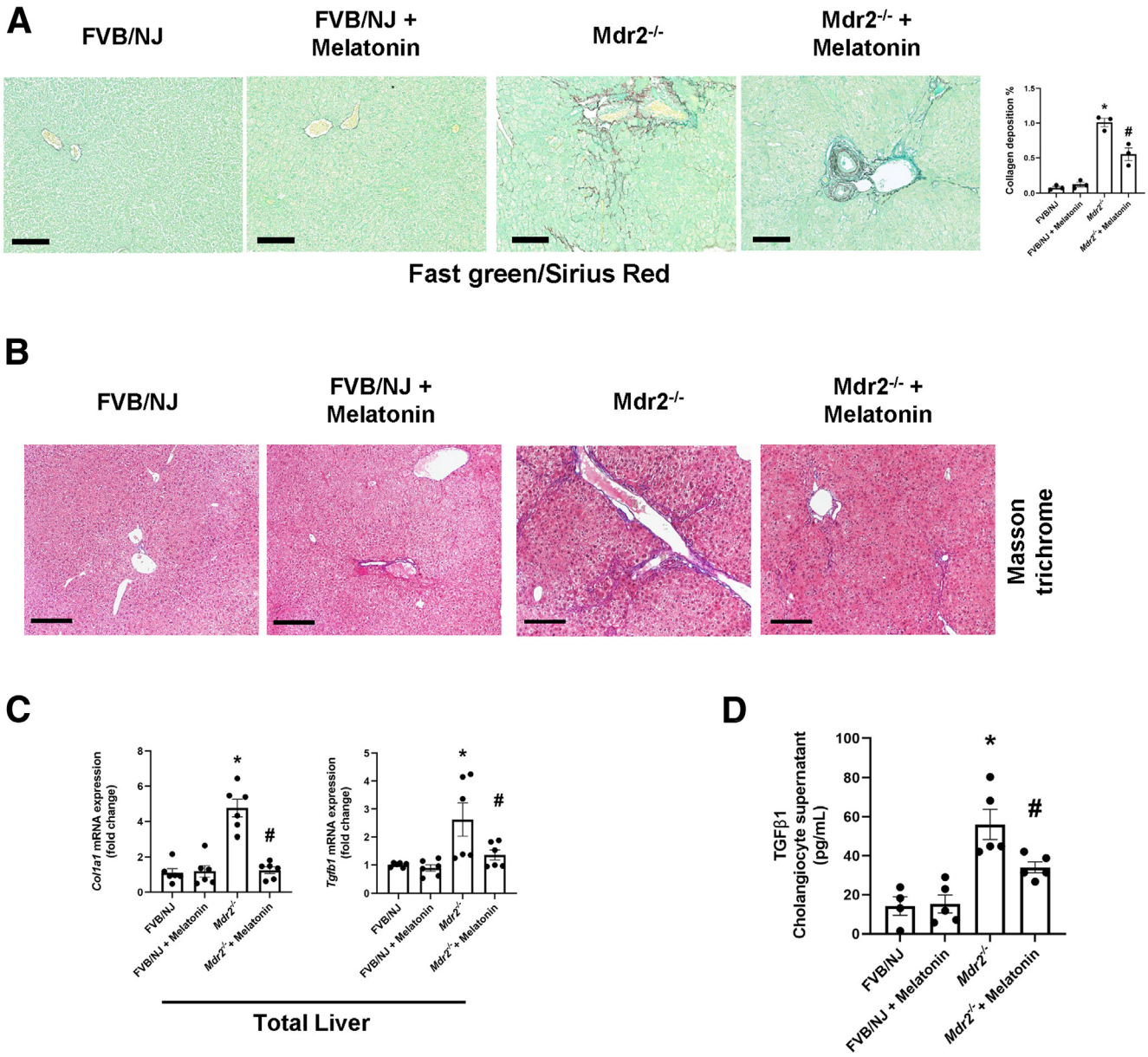

Figure 6. Protective effect of melatonin in liver fibrosis. (*A*) Prolonged administration of melatonin reduced collagen deposition in *Mdr2*$^{-/-}$ mice as shown by Fast Green Sirius red (red) and (*B*) Masson trichrome (blue) staining. Original magnification, 20×; *scale bars*: 200 μm. Data are means ± SEM of slides (completed scanned) from n = 3 different animals per group. (*C*) mRNA expression of *Col1a1* and *Tgfb1* in total liver was decreased in *Mdr2*$^{-/-}$ mice treated with melatonin for 12 weeks; no changes in mRNA expression of the fibrotic markers were observed between WT animals treated with melatonin compared with WT control mice. Data are means ± SEM of 3 evaluations from 3 cumulative preparations of total liver from 4 mice per group. (*D*) *Mdr2*$^{-/-}$ mice have increased levels of TGFβ1 in cholangiocyte supernatant compared with WT groups, and melatonin reduced TGFβ1 levels significantly in *Mdr2*$^{-/-}$ mice. Data are means ± SEM of a duplicate from 4 cumulative preparations of cholangiocytes from 6 mice per group. Each *dot* represents 1 value in data set. $^{*}P < .05$ vs WT; $^{\#}P < .05$ vs *Mdr2*$^{-/-}$ mice.

Measurement of Immunoreactivity/Expression of MT1 in Liver Sections and Cholangiocytes and Expression of Phosphor-Protein Kinase A/cAMP Response Element-Binding Protein/Clock Genes/ miR200b-/*Maspin* (Serpinb5)/*Glutathione-S Transferase Signaling*

Finally, we performed studies aimed to show the effects of melatonin on liver phenotypes of *Mdr2*$^{-/-}$ mice that are associated with changes in the expression of phosphor-protein kinase A (pPKA)/cAMP response element-binding protein (CREB)/clock genes/*miR200b*/*Serpinb5*/glutathione-S transferase (GST) signaling. Through Ingenuity Pathway Analysis software (Qiagen, Germantown, MD) (Figure 10*A*), we postulated that melatonin decreases angiogenesis by improving the activity of the antioxidant enzyme GST (a family of phase II detoxication enzymes) in non–receptor-mediated mechanisms; and by CREB/clock

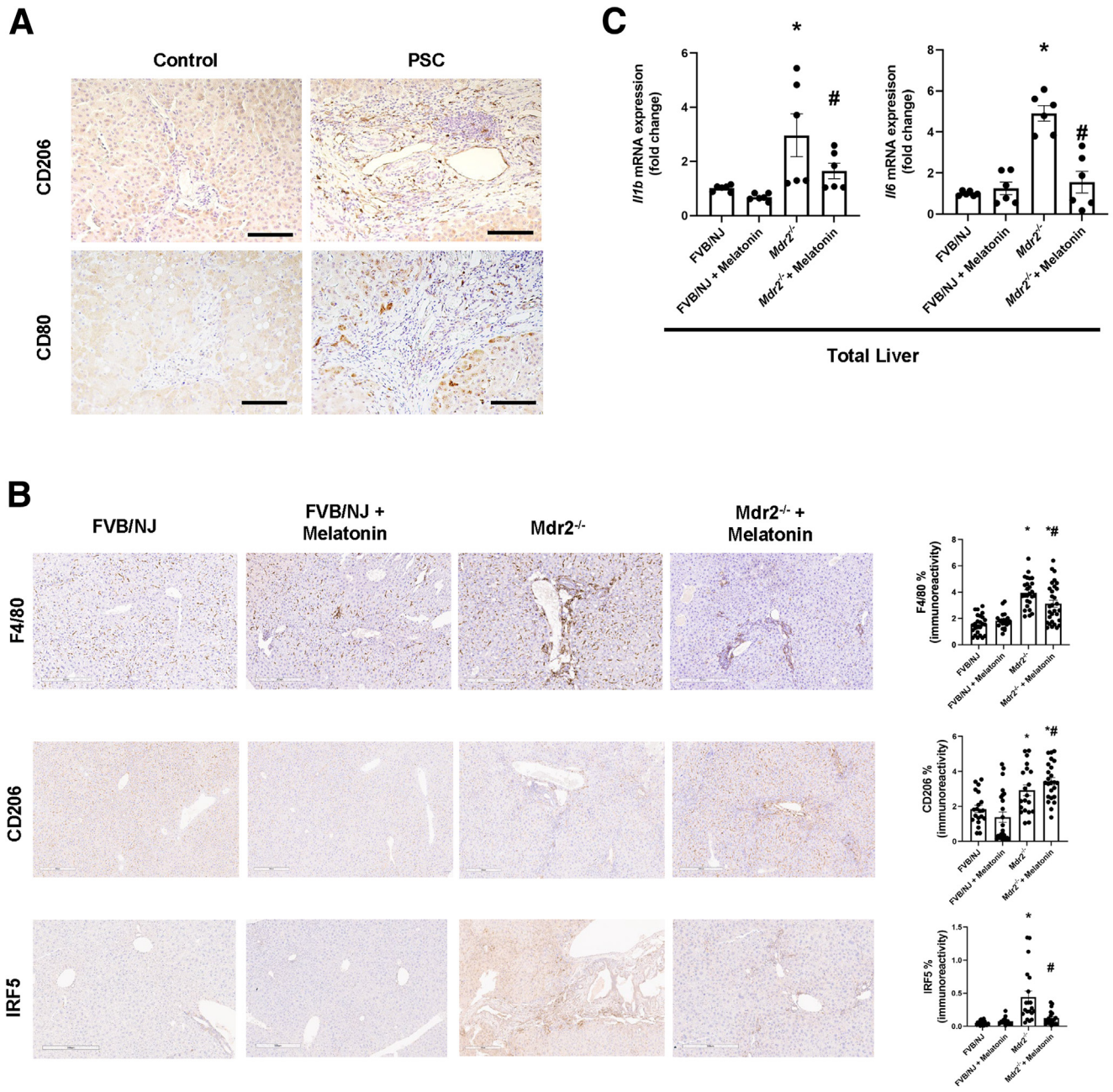

Figure 7. Anti-inflammatory properties of melatonin in Mdr2$^{-/-}$ mice. (*A*) Human PSCs (n = 3) showed increased immunoreactivity of CD206 and CD80 compared with the control group (n = 2). Original magnification, 20×; *scale bars*: 100 μm. (*B*) *Mdr2*$^{-/-}$ mice had increased expression of F4/80 (*upper*), CD206 (*middle*), and interferon-regulatory factor 5 (IRF5) (*lower*). Melatonin decreases the expression of F480 and IRF5 in *Mdr2*$^{-/-}$ mice, but increases the polarization of M2 macrophages in *Mdr2*$^{-/-}$ to relieve peribiliary inflammation. Original magnification, 10×; *scale bars*: 300 μm. (*C*) Quantification data are means ± SEM of 20 nonoverlapping figures from n = 5 different animals per group.[19] mRNA expression of PCR for *Il1b* and *Il6* in total liver were decreased in *Mdr2*$^{-/-}$ mice treated with melatonin compared with the corresponding *Mdr2*$^{-/-}$ mice. Data are means ± SEM of 3 evaluations from 3 cumulative preparations of total liver from 6 mice per groups. Each *dot* represents 1 value in data set. *$P < .05$ vs WT; $^{\#}P < .05$ vs *Mdr2*$^{-/-}$ mice.

genes/*miR200b*/*Serpinb5*/VEGFA through a receptor-mediated mechanism. Previously, we have shown that melatonin reduces biliary damage and liver fibrosis by down-regulation of the MT1/*miR200b*/pPKA/clock genes/angiogenesis axis.[5,8] Several studies have shown the key role of cAMP/PKA signaling in the modulation of biliary homeostasis[25]; and down-regulation of the serine proteinase inhibitor maspin (*Serpinb5*) triggers angiogenesis during tumorigenesis by interaction with GST.[26]

Consistent with the finding that melatonin inhibits biliary hyperplasia in BDL rats by down-regulation of MT1,[8] we showed enhanced biliary immunoreactivity (in liver

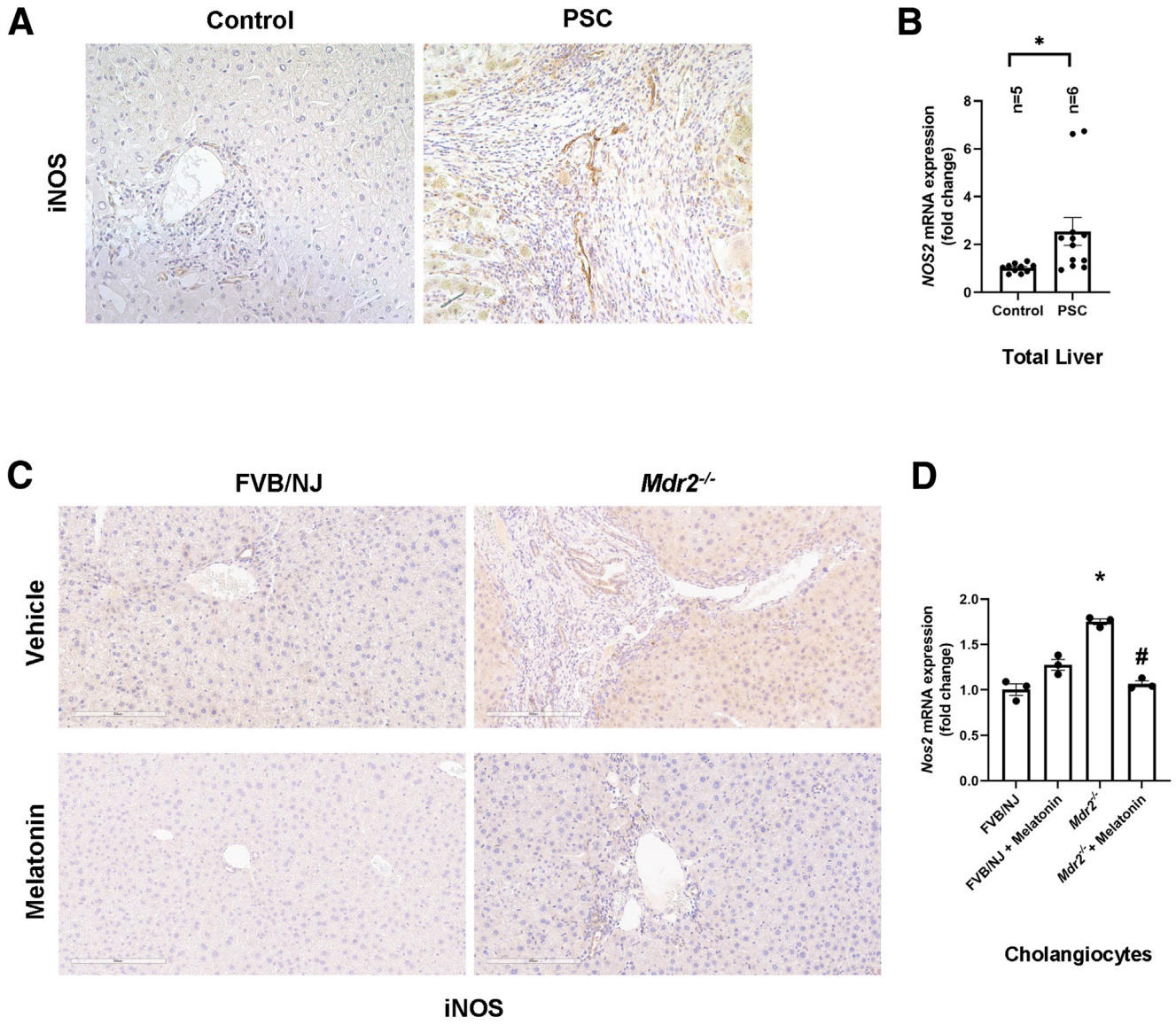

Figure 8. iNOS expression. (*A*) Human PSCs showed increased immunoreactivity of iNOS in both M1 macrophages and cholangiocytes (original magnification, 20×; *scale bars*: 100 μm) and (*B*) mRNA expression of *Nos2* (gene for iNOS) in total liver compared with control group. Data are means ± SEM of 2 evaluations from n = 5 normal and n = 6 PSC samples. This phenotype also was observed in *Mdr2*$^{-/-}$ mice, in which (*C*) the immunoreactivity of iNOS, and (*D*) the mRNA expression of *Nos2* in isolated cholangiocytes were reduced in *Mdr2*$^{-/-}$ treated with melatonin. Data for mRNA expression are means ± SEM of 3 evaluations from 3 cumulative preparations of cholangiocytes from 6 mice per group. Each *dot* represents 1 value in data set. *$P < .05$ vs WT or control; #$P < .05$ vs *Mdr2*$^{-/-}$ mice.

sections) and mRNA expression (in isolated cholangiocytes) of MT1 in 24-week-old *Mdr2*$^{-/-}$ mice compared with WT mice, which was reduced in *Mdr2*$^{-/-}$ mice treated with melatonin for 12 weeks (Figure 10*B* and *C*). In agreement with a previous study,[13] in liver sections there was weak immunoreactivity for MT1 in HSCs, whereas no immunoreactivity for MT1 was observed in hepatocytes (Figure 11). Altogether, these data showed that melatonin decreased the immunoreactivity of MT1 in both cholangiocytes and hepatocytes, but melatonin treatment does not affect MT1 localization or expression in other cell types. Next, we showed enhanced expression of pPKA (brown) in bile ducts (red) by IHC in liver sections and protein expression for phospho-CREB (pCREB)/CREB ratio in cholangiocytes from *Mdr2*$^{-/-}$ mice compared with WT mice, parameters that were reduced in *Mdr2*$^{-/-}$ treated with melatonin (Figure 10*D* and *E*). Together, these data show that melatonin decreases the immunoreactivity of pPKA, which reduces the activation of pCREB to act as a transcription factor in clock gene regulation.[27]

Similar to previous studies,[5,13] we showed enhanced biliary immunoreactivity (in liver sections) and expression (in cholangiocytes) of the clock genes, *PER1*, *CRY1*, *CLOCK*, and *ARNTL*, in *Mdr2*$^{-/-}$ mice compared with WT mice, which

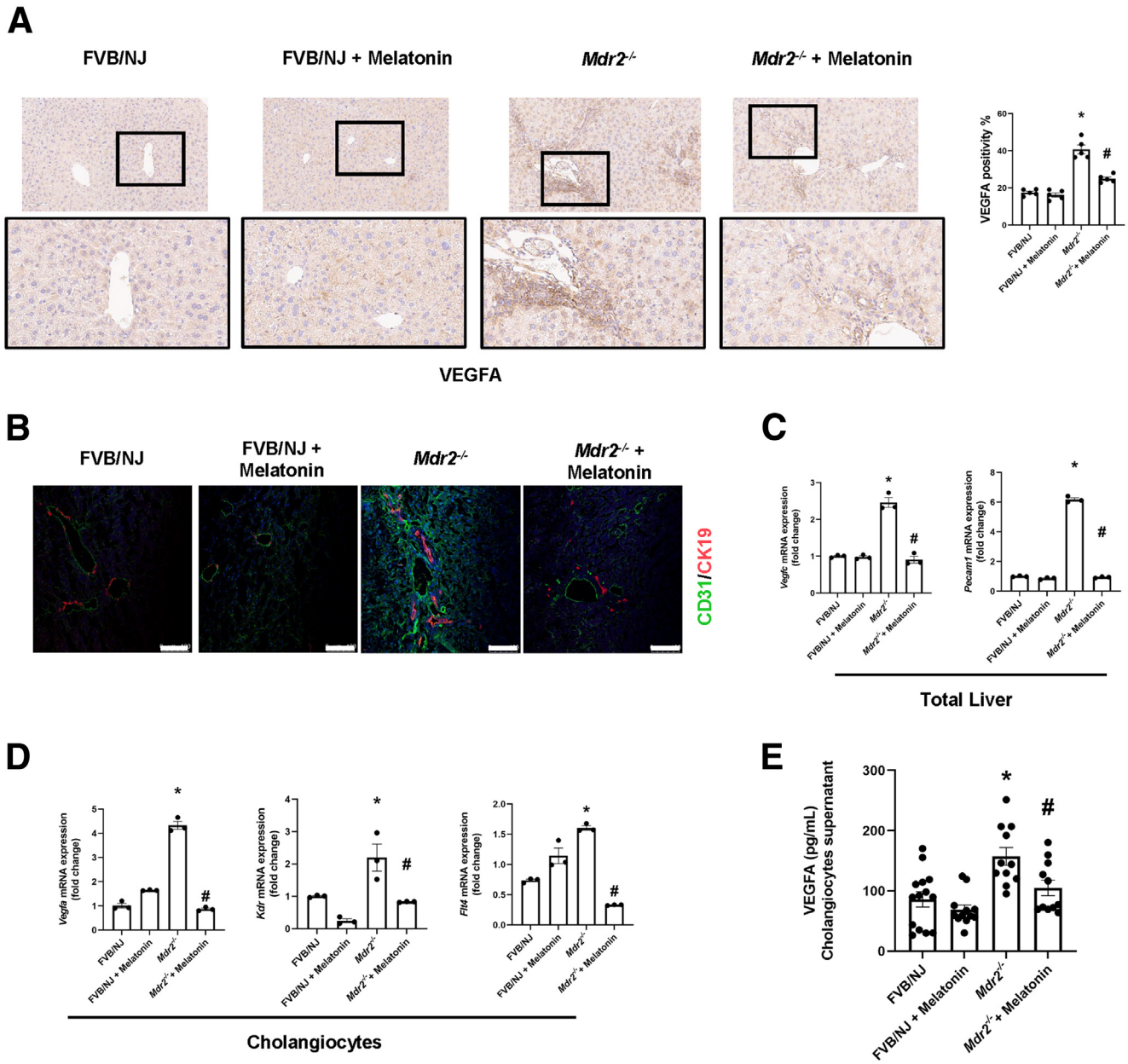

Figure 9. Melatonin acts as an antiangiogenic factor in Mdr2$^{-/-}$ mice. Immunoreactivity of (*A*) VEGFA (*black box*: high-magnification figure) and (*B*) CD31 (green) co-staining with CK19 (red) in paraffin and frozen liver sections, respectively, is increased in *Mdr2*$^{-/-}$ mice compared with the WT group, which is reduced after melatonin treatment. Original magnification, 20×; *scale bars*: 100 μm. (*C*) mRNA expression of angiogenic factors (*Vegfc* and *Pecam1*) in total liver samples (data are means ± SEM of 3 evaluations from 3 cumulative preparations of total liver from 6 mice per group) and (*D*) in isolated cholangiocytes (*Vegfa*, *Kdr*, and *Flt4*; data are means ± SEM of 3 evaluations from 3 cumulative preparations of cholangiocytes from 6 mice per group) was decreased in *Mdr2*$^{-/-}$ mice treated with melatonin for 12 weeks compared with *Mdr2*$^{-/-}$ mice. (*E*) VEGFA cholangiocyte supernatant levels were reduced in *Mdr2*$^{-/-}$ mice after prolonged administration of melatonin. Data are means ± SEM of a duplicate from 4 cumulative preparations of cholangiocytes from 6 mice per group. Each *dot* represents 1 value in data set. $^{*}P < .05$ vs WT; $^{\#}P < .05$ vs *Mdr2*$^{-/-}$ mice.

was decreased in *Mdr2*$^{-/-}$ mice treated with melatonin compared with *Mdr2*$^{-/-}$ mice (Figure 12*A* and *B*). In human histologic samples, we showed enhanced expression in bile ducts of PER1, CRY1, CLOCK, and ARNTL in late-stage PSC compared with healthy control samples (Figure 12*C*). In cholangiocytes from *Mdr2*$^{-/-}$ mice and total liver samples from human PSC samples, we showed decreased levels of *SERPINB5*/maspin, and reduced GST activity; these phenotypes were reversed in the murine groups after melatonin treatment (Figure 13*A* and *B*). Furthermore, both 24-week *Mdr2*$^{-/-}$ mice and late-stage PSC patients showed a significant increase of *miR200b* compared with their corresponding group, which was decreased in *Mdr2*$^{-/-}$ mice treated with melatonin for 12 weeks (Figure 13*D*). Together, these data

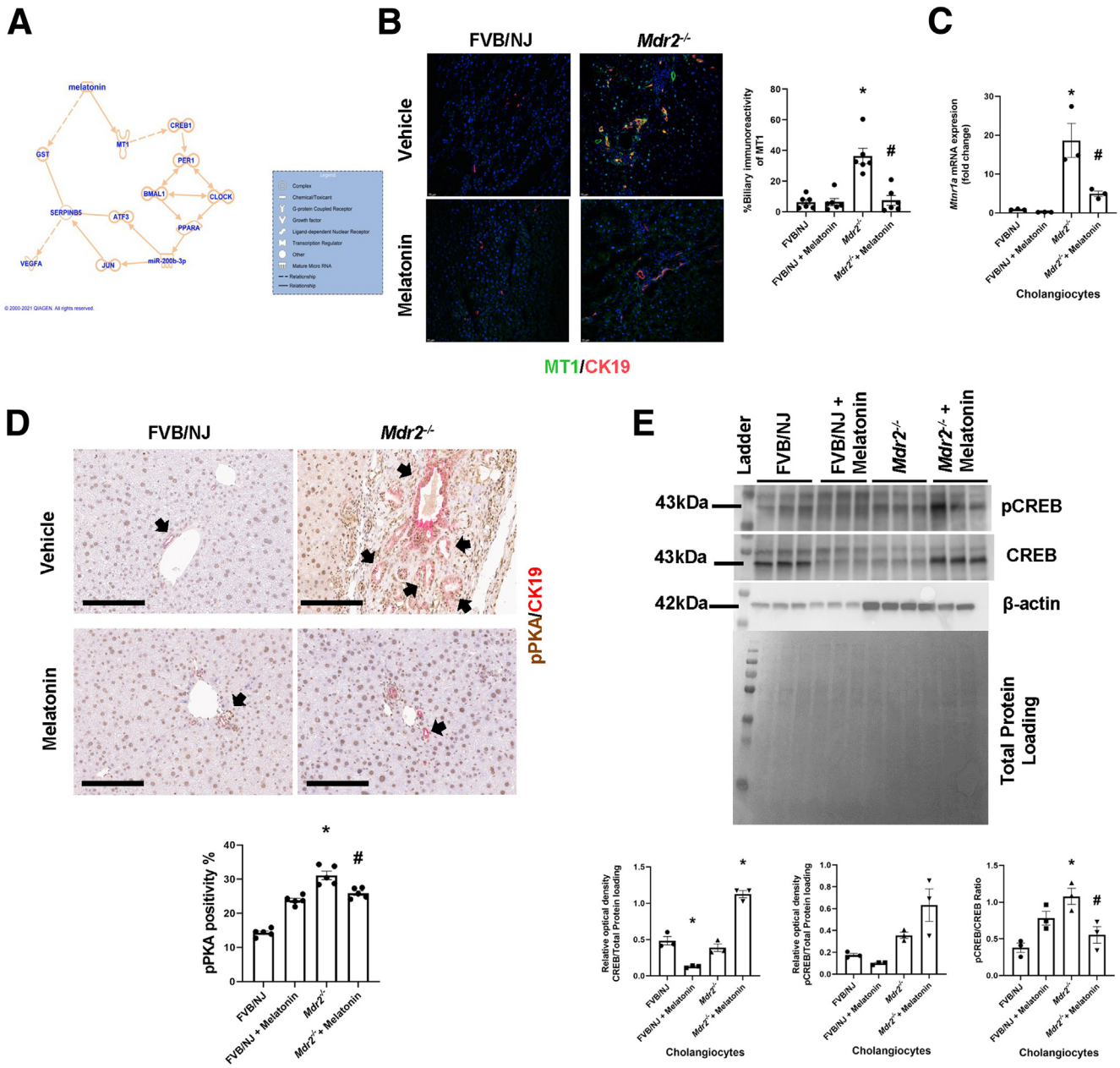

Figure 10. Melatonin interacts with MT1 to down-regulate pPKA/pCREB signaling. (*A*) Ingenuity Pathway Analysis suggested that melatonin may influence VEGF secretion by MT1/pPKA/CREB/clock genes/*miR200b*/Maspin signaling. (*B*) Enhanced biliary immunoreactivity (in liver sections, original magnification, 20×; *scale bars*: 20 μm; data are means ± SEM of 6 pictures from n = 3 different animals per group) and (*C*) mRNA expression (in isolated cholangiocytes) of *Mtnr1a* were observed in *Mdr2*$^{-/-}$ compared with WT mice, which was reduced in *Mdr2*$^{-/-}$ mice treated with melatonin. Data are means ± SEM of 3 evaluations from 3 cumulative preparations of cholangiocytes from 6 mice per group. (*D*) Immunoreactivity of pPKA is reduced in *Mdr2*$^{-/-}$ mice treated with melatonin for 12 weeks. Original magnification, 20×; *scale bars*: 100 μm *black arrows* showed the pPKA-bile duct positivity. (*E*) The pCREB/CREB ratio in isolated cholangiocytes showed increased activation of pCREB in *Mdr2*$^{-/-}$ mice compared with WT. Its activation was reduced after melatonin treatment. Both CREB and pCREB were normalized with total protein loading (Pounce S staining). Data are means ± SEM of 3 evaluations from cumulative preparations of cholangiocytes from 6 mice per group. Each *dot* represents 1 value in data set. $^{*}P < .05$ vs WT; $^{\#}P < .05$ vs *Mdr2*$^{-/-}$ mice.

showed that melatonin may be linked to *miR200b* by reducing its expression through the MT1/clock gene axis in a murine PSC model, as well as there is an association between *mir200b* and angiogenesis through maspin/GST signaling.

In Vitro Effect of Melatonin on Biliary Phenotypes

We observed that the PSC cholangiocyte cell line is approximately 94% positive for CK19 showing an epithelial origin (Figure 14*B*). Moreover, there was no positive immunoreactivity for hepatocytes, macrophages, or

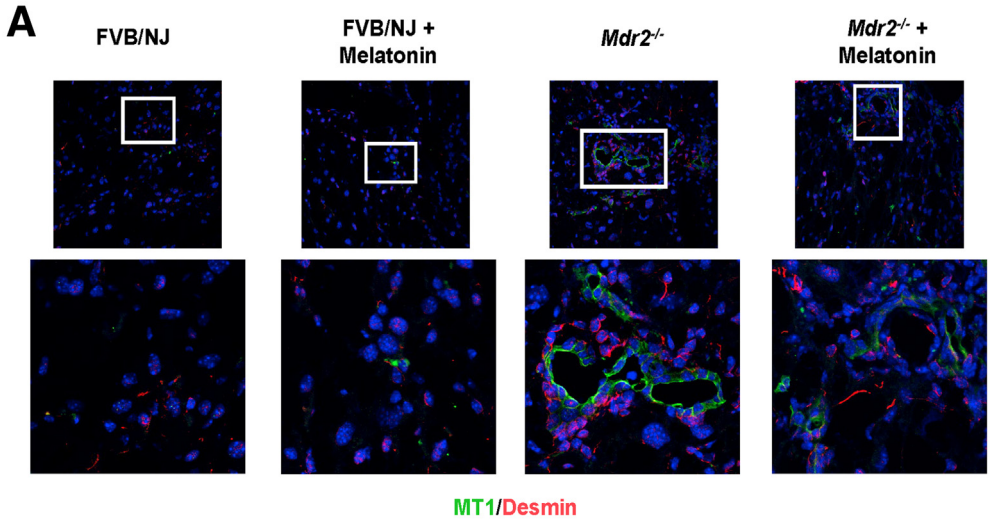

Figure 11. MT1 expression in different cell lines. By immunofluorescence, (*A*) HSCs (red, desmin) showed low expression of MT1 (green) in *Mdr2*$^{-/-}$ mice compared with WT, which was reduced in *Mdr2*$^{-/-}$ mice treated with melatonin. (*B*) There was no colocalization of MT1 (green) with the hepatocytes (red, HNF4α) in the experimental groups. Original magnification, 40×; (*upper side*). The *white box* shows a high-magnification picture, 100×.

endothelial cell markers and less immunoreactivity of HSCs in the PSC isolated cell lines (Figure 14*C*). Melatonin-treated PSC cholangiocyte cells have reduced immunoreactivity and mRNA expression of *MTNR1A* and clock genes (PER1, CRY1, CLOCK, and ARNTL) compared with the vehicle-treated P92–PSC control group (Figure 15). Finally, mRNA expression of proliferative, senescence, fibrotic, and angiogenic markers, as well as *miR200b*, are decreased significantly in the melatonin–PSC cholangiocyte cell line compared with the vehicle-treated PSC control group (Figure 16).

Discussion

In the present study, we showed that prolonged melatonin administration to *Mdr2*$^{-/-}$ mice ameliorates PSC phenotypes, such as biliary senescence and collagen deposition. No changes in liver phenotypes were observed in WT mice treated with melatonin and melatonin did not induce pathologic changes in other organs. The beneficial effects of melatonin on liver damage were associated with reduced liver inflammation and angiogenesis. Our findings support the beneficial effects of long-term melatonin exposure (12 weeks of treatment) by acting as an antiproliferative,[28] anti-inflammatory,[29] and anti-angiogenic agent[30] in cholestatic liver diseases, and the amelioration of biliary senescence and release of senescence-associated secretory phenotype such as TGFβ1.[3,14,31] Furthermore, we observed that long-term melatonin treatment does not induce any negative morphologic changes in other organs. Our data are supported by a previous study showing that short-term melatonin administration in severely ill human beings is considered safe, and long-term administration (24 weeks) does not induce serious adverse events.[32] Furthermore, in a pilot study, 3-month administration of melatonin to patients with nonalcoholic steatohepatitis reduced plasma levels of liver enzymes and lipids through increased melatonin serum levels.[33] These observations and the evidence of melatonin's strong antioxidant and anti-inflammatory effects in the experimental setting prompt studies to determine the efficacy of this molecule as a therapeutic for human cholangiopathies.[34]

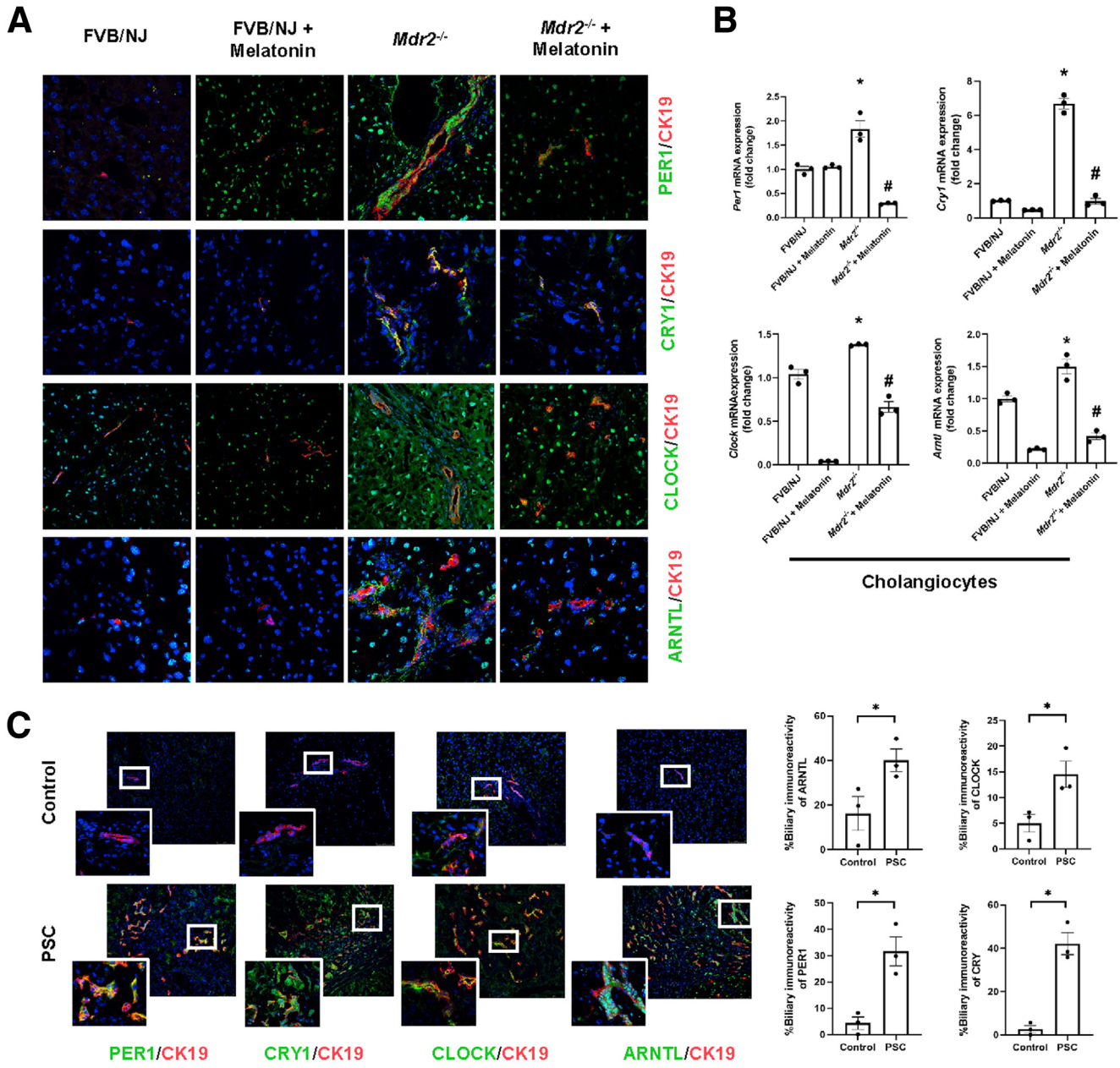

Figure 12. Melatonin resynchronized clock gene expression in Mdr2$^{-/-}$ mice. (*A*) By immunofluorescence, *Mdr2*$^{-/-}$ mice have increased immunoreactivity of clock genes (green) compared with WT, which was reduced in *Mdr2*$^{-/-}$ mice treated with melatonin for 12 weeks. Original magnification, 40×. (*B*) *Per1*, *Cry1*, *Clock,* and *Arntl* mRNA expression from isolated cholangiocytes of *Mdr2*$^{-/-}$ mice treated with melatonin for 12 weeks were decreased compared with *Mdr2*$^{-/-}$ mice. Each *dot* represents 1 value in data set. Data are means ± SEM of 3 evaluations from 3 cumulative preparations of cholangiocytes from 6 mice per group. $^{*}P < .05$ vs WT; $^{\#}P < .05$ vs *Mdr2*$^{-/-}$ mice. (*C*) Immunofluorescence staining for clock genes (green) co-stained for CK19 (red) showed increased immunoreactivity in PSC patients compared with the normal group. Original magnification, 40×; *scale bar*: 10 μm. *White box*: high-magnification picture, 100×. Data are means ± SEM of 3 pictures from n = 3 different human samples per group. $^{*}P < .05$ vs control group.

The secretory and proliferative functions of cholangiocytes are regulated by several gastrointestinal hormones and neuropeptides such as secretin and melatonin.[31,35] We have previously shown that, in the cholestatic rat model of BDL, MT1 and MT2 receptors are up-regulated together with the clock genes, CLOCK, BMAL1, CRY1, and PER1; and that short-term (1 week) melatonin treatment reduces BDL-induced biliary hyperplasia, liver damage, and clock gene expression.[8] In the same study, experiments performed with Luzindole (a receptor antagonist for MT1 and MT2 that has approximately 11- to 25-fold greater affinity for MT2 compared with MT1)[36] or 4-phenyl-2-propionamidotetralin (4-P-PDOT, MT2 receptor antagonist that is >300-fold more selective for MT2 than MT1)[37]

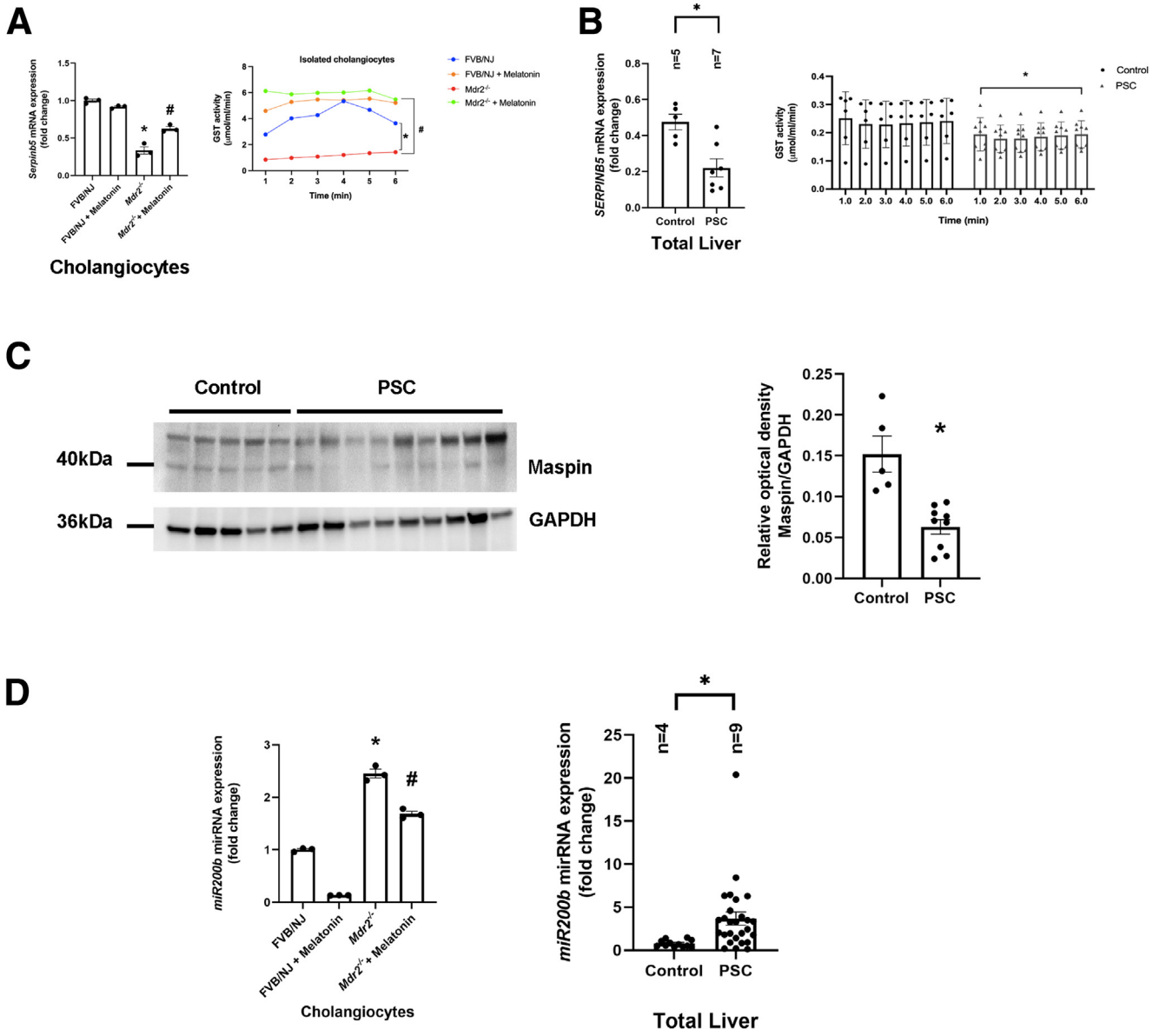

Figure 13. Pleiotropic effects of melatonin are mediated by miR-200b/maspin signaling. (*A*) *Serpinb5* (*left*) mRNA expression and GST activity from isolated cholangiocytes of *Mdr2*$^{-/-}$ mice treated with melatonin for 12 weeks were increased compared with *Mdr2*$^{-/-}$ mice. Data are means ± SEM of 3 evaluations from 3 cumulative preparations of cholangiocytes from 6 mice per group. (*B*) Human PSCs showed decreased mRNA levels of *SERPINB5* (*left*), and reduced GST activity (*right*) compared with the control group. (*C*) This phenotype was confirmed by immunoblot of maspin in total liver human samples. Data for mRNA expression are means ± SEM of 2 evaluation from n = 5 normal and n = 7 PSC samples. Data for GST activity are means ± SEM of 2 evaluations from n = 6 normal and n = 6 PSC samples. Data for immunoblots are means ± SEM of n = 5 normal and n = 9 PSC samples. (*D*) *Mdr2*$^{-/-}$ mice have increased mRNA expression of *miR200b* in both murine (*left*) and human PSC samples (*right*), which was reduced with melatonin treatment; no changes in *miR200b* expression were observed between WT animals treated with melatonin compared with WT control mice. Data are means ± SEM of 3 evaluations from 3 cumulative preparations of cholangiocytes from 6 mice per group. Data for mRNA expression are means ± SEM of 2 evaluation from n = 4 normal and n = 9 PSC samples. Each *dot* represents 1 value in data set. *$P < .05$ vs WT or control; #$P < .05$ vs *Mdr2*$^{-/-}$ mice. GAPDH, glyceraldehyde-3-phosphate dehydrogenase.

allowed us to determine that the MT1 receptor likely mediates the beneficial effects of melatonin.[8] In separate studies in BDL and *Mdr2*$^{-/-}$ mice, we provided conclusive evidence that melatonin improves liver phenotypes through down-regulation of MT1 (a receptor subtype expressed mainly by cholangiocytes). In contrast, knockout of MT2 triggers biliary damage and liver fibrosis through GPR50/TGFβR1 signaling.[14]

Higher nocturnal expression of AANAT in rodents and the involvement of CREB activation in melatonin synthesis have been described.[38] Furthermore, it has been shown that *PER1*$^{-/-}$ mice show increased nocturnal AANAT transcription

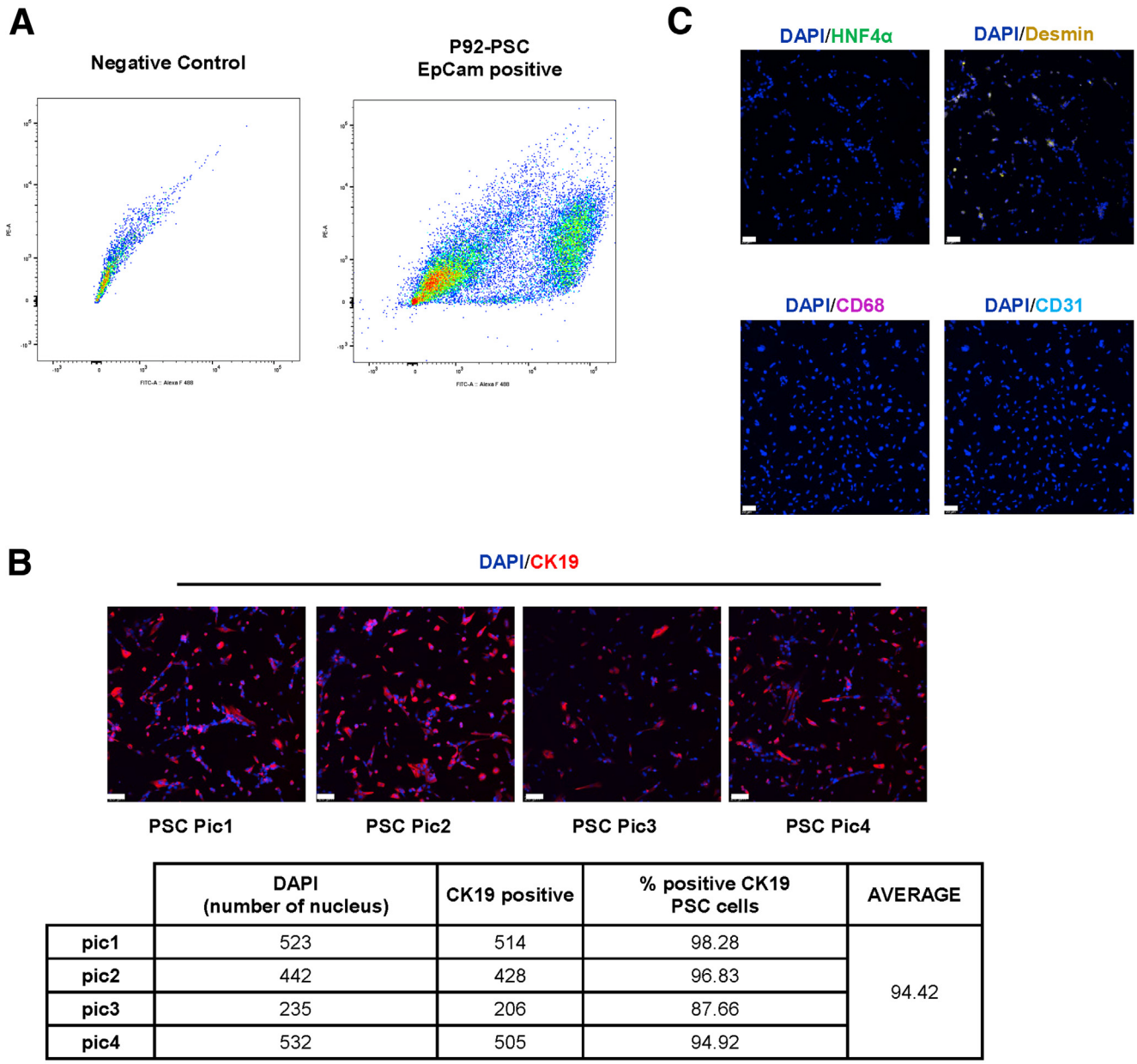

	DAPI (number of nucleus)	CK19 positive	% positive CK19 PSC cells	AVERAGE
pic1	523	514	98.28	94.42
pic2	442	428	96.83	
pic3	235	206	87.66	
pic4	532	505	94.92	

Figure 14. (*A*) Fluorescence-activated cell sorting plot represents the percentage of the EpCAM-positive cell in H69 (control) and PSC cells (*right*). (*B*) Representative image of PSC cell line (*upper*, n = 4) and table (*lower*) to show the purity of the cell lines (94.42%). Original magnification, 10×; *scale bars*: 20 μm. (*C*) Evaluation of other cell lines to determine contamination, such as hepatocytes (HNF4α, green), HSCs (desmin, yellow), CD68 (macrophages, magenta), and endothelial cells (CD31, cyan). Original magnification, 10×; *scale bars*: 20 μm. DAPI, 4′,6-diamidino-2-phenylindole; EpCAM, Epithelial cell adhesion molecule; FITC-A, Fluorescein isothiocyanate.

in the pineal gland[39] and the role of BMAL1–CLOCK heterodimer in triggering biliary AANAT expression.[40] Together with our data, these results conclude that increased clock gene expression in *Mdr2*$^{-/-}$ mice increases the expression of AANAT in cholangiocytes. After melatonin administration in the cholestatic murine model, we proposed that the clock system is restored along with AANAT expression. Because AANAT is expressed mainly by cholangiocytes and at lower levels by hepatocytes (but not HSCs)[13]; and melatonin serum levels are decreased markedly in 24-week-old *Mdr2*$^{-/-}$ mice, our data support the concept that melatonin administration ameliorates biliary/liver phenotypes by both paracrine (enhanced secretion of melatonin by the pineal gland)[12,13,35] and autocrine mechanisms (by increased melatonin biliary secretion)[12,13,35] as evidenced by enhanced levels of melatonin in serum. Interestingly, the chronic administration of melatonin to WT and *Mdr2*$^{-/-}$ mice did not change the hepatic localization of AANAT, further supporting the concept that enhanced biliary melatonin secretion may be a key factor modulating biliary/liver

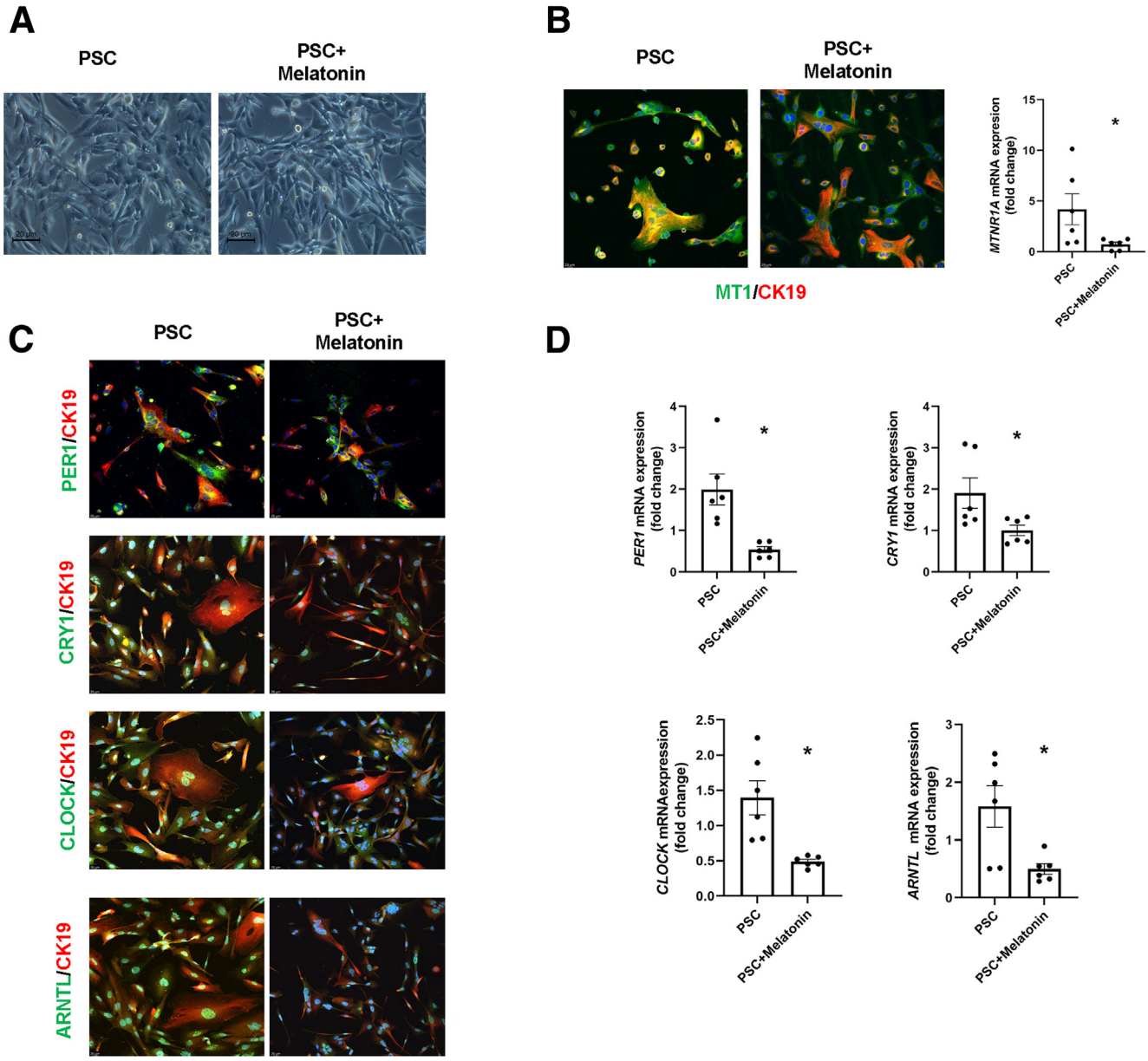

Figure 15. Melatonin influences the phenotype of isolated P92-PSC. (*A*) Morphologic shapes of human isolated PSC cell line. *Scale bars*: 20 μm. (*B*) By immunofluorescence and qPCR, the MT1 and (*C* and *D*) clock genes (PER1, CRY1, CLOCK, and BMAL1) are decreased in isolated PSC cell lines treated with melatonin compared with vehicle-treated PSC cells. Original magnification, 20×; *scale bars*: 20 μm. Data are means ± SEM of 2 evaluations from 3 cumulative preparations of in vitro experiments. Each *dot* represents 1 value in data set. *$P < .05$ vs PSC.

damage. Consistent with previous studies,[8,14] the effects of melatonin were associated with decreased biliary expression of MT1, the receptor by which melatonin exerts its therapeutic effects in the liver by down-regulation of cAMP/PKA signaling.[14] Several studies in other cell systems have shown that melatonin effects are mediated by interaction with the MT1 receptor.[41,42] MT1–melatonin interaction also ameliorates liver injury caused by alcohol gastric perfusion reducing lipid peroxidation through down-regulation of cAMP, but enhanced the activity of AMPK.[41] Moreover, melatonin–MT1 interaction inhibits insulin secretion in rat insulinoma cells and mouse pancreatic islets through decreased phosphorylation of CREB protein.[43] The finding that melatonin amelioration of liver damage is mediated by down-regulation of cAMP signaling supports the concept that this transduction pathway plays a vital role in the homeostasis of biliary functions.[44,45] Because cAMP/phosphorylated extracellular signal-related kinase (pERK1/2)/TGFβ1 signaling plays a key role in the modulation of biliary phenotypes and liver fibrosis, and because MT1 receptors are expressed mainly by cholangiocytes,[5,14] our findings support the concept that melatonin effects on liver

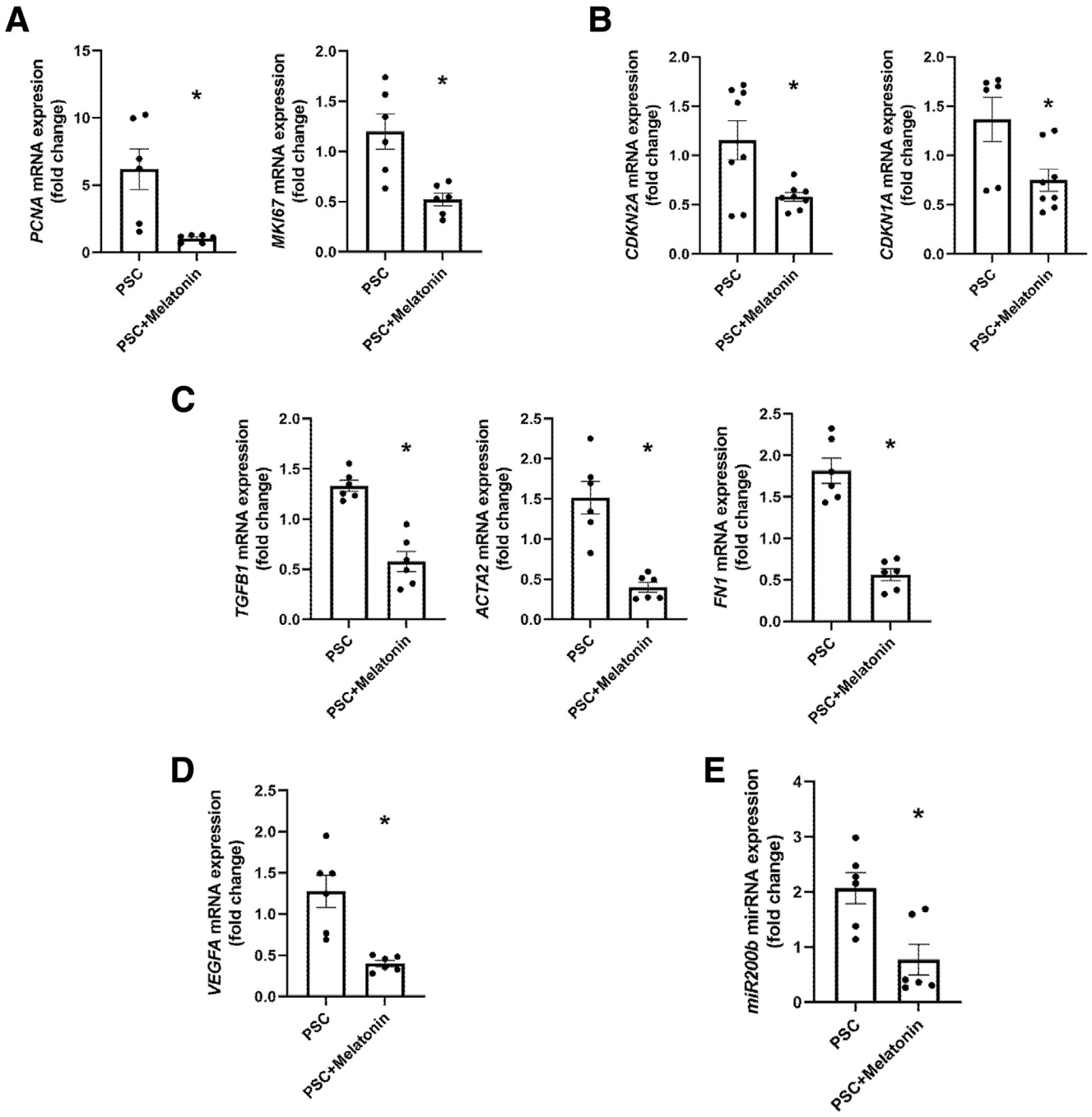

Figure 16. Isolated P92-PSC phenotype. (*A*) Proliferative (*PCNA*, *KIM67*), (*B*) senescence (*CDKN1A*, *CDKN2A*), (*C*) fibrotic (*TGFB1, FN1*, and *ACTA2*), and (*D*) angiogenic (*VEGFA*) markers, as well as (*E*) *miR200b* is decreased in isolated PSC cell lines treated with melatonin compared with vehicle-treated PSC cells. Data are means ± SEM of 2 evaluations from 3 cumulative preparations of in vitro experiments. Each *dot* represents 1 value in data set. *$P < .05$ vs PSC.

phenotypes are mediated by changes in cholangiocyte signaling, which affect the functions of adjacent cholangiocytes, Kupffer cells, and HSCs by paracrine pathways.[14,46–48] However, melatonin actions on cholangiocytes, Kupffer cells, and HSC phenotypes may be regulated by receptor-independent mechanisms because previous studies have shown that melatonin acts as an antioxidant, increasing GST activity.[22,49] Regarding this latter point, 1 study underscored the role of lipid peroxidation (characteristically in the periportal area) and reduced antioxidant activity in human PSCs as an essential process in the progressing pathogenesis of this disease.[50]

Several studies have shown that neo-angiogenesis regulates biliary damage, liver inflammation, and fibrosis during the progression of liver diseases in both rodent models of cholestasis and human samples,[5,24,51] and the

Table 2. Patient Information

Groups	Sample ID	Company	Gender	Age, *y*	Blood type	Ethnicity	Sample
Control	H1255	XenoTech	Female	56	N/A	African American	Liver
	H1293	XenoTech	Female	52	N/A	Caucasian	Liver
	H1296	XenoTech	Male	46	N/A	Caucasian	Liver
	H1299	XenoTech	Female	17	N/A	Caucasian	Liver
	EB66	Indiana University (IU) Health University Hospital	Male	46	O	Unknown	Liver
	EB92	IU Health University Hospital	Unknown	Unknown	Unknown	Unknown	Liver
	EB125	IU Health University Hospital	Male	35	A	Unknown	Liver
	EB126	IU Health University Hospital	Male	43	O	Unknown	Liver
PSC	PSC1	IU Health University Hospital	Unknown	Unknown	Unknown	Unknown	Liver
	EB29	IU Health University Hospital	Female	59	O	Unknown	Liver
	EB37	IU Health University Hospital	Male	33	A	Unknown	Liver
	EB43	IU Health University Hospital	Female	45	O	Unknown	Liver
	EB62	IU Health University Hospital	Male	61	O	Unknown	Liver
	EB71	IU Health University Hospital	Male	38	O	Unknown	Liver
	EB80	IU Health University Hospital	Female	56	O	Unknown	Liver
	EB94	IU Health University Hospital	Male	55	O	Unknown	Liver
	EB97	IU Health University Hospital	Male	60	A	Unknown	Liver
	EB105	IU Health University Hospital	Male	32	O	Unknown	Liver

miR200b/TGFβ1 signaling axis (up-regulated in BDL and *Mdr2*$^{-/-}$ mice and down-regulated by melatonin)[4,5,46] regulates biliary damage and liver fibrosis in cholangiopathies. Based on this background, we performed experiments that showed that the expression of the *miR200b*/angiogenesis axis increases in our mouse models of cholestasis and human PSC samples, but was down-regulated in *Mdr2*$^{-/-}$ mice treated with melatonin. We show that human PSC samples and *Mdr2*$^{-/-}$ mice had decreased expression/activity of maspin/GST and increased expression of *miR200b*. Melatonin reduces angiogenesis through receptor and non–receptor-mediated mechanisms. Specifically, melatonin interaction with MT1 restores the circadian rhythm and down-regulates *miR200b*, enhancing maspin expression and GST activity presumably by a non–receptor-mediated mechanism. Supporting our findings, several studies have shown the therapeutic effects of maspin (*SerpinB5*) and its role as an antiangiogenic factor in different cancer models.[52,53] In addition, when maspin is expressed endogenously, there is increased GST activity, which decreases VEGF-dependent angiogenesis in human prostatic carcinoma cell lines.[26] Supporting the importance of melatonin in regulating liver angiogenesis, studies have shown that melatonin reduces tumor angiogenesis in a renal adenocarcinoma murine model[54] and VEGF serum levels in patients with metastatic diseases.[55]

In the last sets of experiments, we aimed to evaluate the role of melatonin in the modulation of clock genes, which several studies have shown to play a key role in early and late-stage liver diseases.[9,35,56] For example, a study showed dysregulation of circadian rhythm in primary biliary cholangitis patients associated with a disturbance of sleep–wake patterns.[56] Furthermore, melatonin stimulates mitophagy, with a high number of mitophagosomes in hepatocytes, through changes in circadian clocks in a mouse model of viral-induced fulminant hepatraphiic failure.[57] Dysregulation of the circadian rhythm regulates hepatic lipid metabolism, gut microbiota, and gallstone formation in a mouse model of a lithogenic diet.[58] Parallel to our previous work and the present study showing up-regulation of selected clock genes during cholestasis,[8,13] an in vitro study has shown that alcohol-induced intestinal hyperpermeability (that triggers liver injury) is associated with increased Clock and Per2 circadian expression. In contrast, the knockdown of these clock genes prevents alcohol-induced permeability.[59] In addition, a study showed the role of the circadian clock in regulating angiogenesis developments by modulation of VEGF in developing zebrafish.[60] The increase in biliary damage, liver fibrosis, angiogenesis, and clock gene expression (observed in BDL rats subjected to pinealectomy or prolonged exposure to light and in a human PSC cholangiocyte line) was reduced by melatonin treatment.[13] Moreover, the inhibitory effect of melatonin on BDL-induced biliary damage was associated with decreased clock gene expression.[8] In summary, our findings support the concept that the inhibition of biliary damage during chronic liver diseases may be performed by a combination of both melatonin with current antiangiogenic therapy,[51] which could be an essential therapeutic approach for the management of cholangiopathies such as PSC.

Materials and Methods

Unless otherwise indicated, reagents were purchased from Sigma-Aldrich Chemical Co. (St. Louis, MO). Total liver RNA was extracted with TRIzol reagent from Sigma Life Science (Burlington, MA); RNA isolation from isolated cholangiocytes was performed with the mirVANA miRNA isolation Kit (AM1561; Invitrogen, Waltham, MA). The iScript cDNA Synthesis Kit and iTaq Universal SYBR Green Supermix were purchased from Bio-Rad Laboratories (Hercules, CA). The Real-Time PCR machine used was the Applied Biosystems QuantStudio 7 Flex (Bedford, MA), and data were analyzed with the QuantStudio real-time PCR software v1.3. The mouse and human PCR primers were purchased from Qiagen (Germantown, MD) (Table 2). The

Table 3. List of PCR Primers

Gene	Species	Reference sequence	Company
Aanat	Mouse	NM_009591	Qiagen
Arntl	Mouse	NM_007489	Qiagen
Cdkn1a (p21)	Mouse	NM 007669	Qiagen
Cdkn2a (p16)	Mouse	NM 009877	Qiagen
Col1a1	Mouse	NM 007742	Qiagen
Clock	Mouse	NM_007715	Qiagen
Cry1	Mouse	NM_007771	Qiagen
Flt4 (VEGFR3)	Mouse	NM_008029	Qiagen
Il1b	Mouse	NM_008361	Qiagen
Il6	Mouse	NM_031168	Qiagen
Kdr (VEGFR2)	Mouse	NM_010612	Qiagen
miR200b	Mouse	MI0000342	ThermoFisher
MTNR1A[a]	Mouse	NM_008639	Designed by us
Nos2	Mouse	NM_001313921	Qiagen
Pecam1	Mouse	NM_008816	Qiagen
Per1	Mouse	NM_011065	Qiagen
Rps18	Mouse	NM_011296	Qiagen
RNAU6	Mouse	NR_004394	ThermoFisher
Serpinb5 (maspin)	Mouse	NM_009257	Qiagen
Tgfb1	Mouse	NM 011577	Qiagen
Vegfa	Mouse	NM 009505	Qiagen
Vegfc	Mouse	NM 009506	Qiagen
AANAT	Human	NM 001088	Qiagen
ACTB	Human	NM 001101	Qiagen
ARNTL	Human	NM 001178	Qiagen
ACTA2	Human	NM 001613	Qiagen
CDKN1A	Human	NM 000389	Qiagen
CDKN2A	Human	NM 000077	Qiagen
CLOCK	Human	NM 004898	Qiagen
CRY1	Human	NM 004075	Qiagen
FN1	Human	NM 002026	Qiagen
GAPDH	Human	NM 002046	Qiagen
MTNR1A	Human	NM 005958	Qiagen
NOS2	Human	NM 000625	Qiagen
PER1	Human	NM 002616	Qiagen
TGFB1	Human	NM 000660	Qiagen
SERPINB5	Human	NM 002639	Qiagen
VEGFA	Human	NM 003376	Qiagen

p21, cyclin-dependent kinase inhibitor 1A.
[a]The mouse Mtnr1a primers were designed in our laboratory (sequence: forward: TGTGTACCGCAACAAGAAGC, reverse: GTCAGCACCAAGGGATAAGG).

antibodies used are listed in Table 3. The stripping buffer used for immunoblots were Restore Western Blot Stripping Buffer and the substrate used was SuperSignal West Femto Maximum Sensitivity Substrate, both were purchased from ThermoFisher Scientific, Inc (Waltham, MA).

All the immunofluorescence staining in liver frozen sections (6-μm thick) was analyzed by the SP8 confocal microscope platform from Leica Microsystems (Leica Microsystems, Inc, Buffalo Grove, IL) and immunohistochemistry in paraffin liver sections (4-μm thick) in both mouse and human samples, which were evaluated by the Leica Aperio AT2 (Aperio Scanscope CS System, Leica Biosystems, Milan, Italy) and the Olympus BX-51 light microscope with a DP27 Microscope Digital Camera from Olympus (Center Valley, PA) in a blinded fashion for mouse and human samples, respectively.

Table 4. List of Antibodies

Antibodies	Application	Description	Catalog number	Company
AANAT	IHC	Rabbit polyclonal	ab3505	Abcam (Cambridge, UK)
ARNTL	IF	Rabbit polyclonal	PA1-523	Invitrogen (Waltham, MAMassachusetts, US)
B-actin	WB	Mouse monoclonal	Sc-47778	Santa Cruz Biotechnology, (Dallas, TX)
CD206	IHC	Rabbit Monoclonal	24595	Cell Signaling (Danvers, MA)
CD31	IF	Rat monoclonal	ab7388	Abcam (Cambridge, UK)
CD80	IHC	Rabbit polyclonal	ab64116	Abcam (Cambridge, UK)
CK19	IHC/IF	Rat monoclonal	TROMA III	Developmental Studies Hybridoma Bank (Iowa City, IA)
CLOCK	IF	Rabbit polyclonal	PA1-520	Invitrogen (Waltham, MA)
Collagen 1	IF	Rabbit polyclonal	ab21286	Abcam (Cambridge, UK)
CREB (ser133)(87G3)phospho-	WB	Rabbit monoclonal	9198S	Cell Signaling (Danvers, MA)
CREB total-	WB	Rabbit monoclonal	9197S	Cell Signaling (Danvers, MA)
CRY1	IF	Rabbit polyclonal	PA1-527	Invitrogen (Waltham, MA)
Desmin	IF	Goat polyclonal	AF3844	R&D Systems (Minneapolis, MN)
F4/80	IHC	Rabbit monoclonal	70076S	Cell Signaling (Danvers, MA)
GAPDH-HRP (conjugated)	WB	Mouse monoclonal	51332S	Cell Signaling (Danvers, MA)
HNF4A	IF	Goat polyclonal	LS-C758303	LifeSpan Biosciences (Seattle, WA)
iNOS	IHC	Rabbit polyclonal	ab15323	Abcam (Cambridge, UK)
IRF5	IHC	Rabbit monoclonal	Ab181553	Abcam (Cambridge, UK)
Maspin (T50)	WB	Rabbit polyclonal	9117S	Cell Signaling (Danvers, MA)
MT1	IF	Rabbit polyclonal	Orb11085	biorbyt (Cambridge, UK)
P16	IF	Rabbit polyclonal	Ab189034	Abcam (Cambridge, UK)
PCNA	IHC	Rabbit monoclonal	13110S	Cell Signaling (Danvers, MA)
PER1	IF	Rabbit polyclonal	PA1-524	Invitrogen (Waltham, MA)
pPKA	IHC	Rabbit polyclonal	9621S	Cell Signaling (Danvers, MA)
VEGFA	IHC	Rabbit monoclonal	ab52917	Abcam (Cambridge, UK)

AANAT, aralkyl amine N-acetyltransferase; ARNTL, Arnt-like protein-1; CLOCK, circadian locomotor output cycles kaput; CRY1, cryptochrome circadian regulator 1; GAPDH, glyceraldehyde-3-phosphate dehydrogenase; HRP, horseradish peroxidase; IF, immunofluorescence; IHC, immunohistochemistry; IRF5, interferon regulatory factor 5; Mdr2, multidrug resistance protein 2; PER1, period circadian clock 1; p16, cyclin-dependent kinase inhibitor 2A; PER1, period circadian regulator 1; WB, Western blot.

Measurement of Immunoreactivity/Expression of AANAT in Liver Sections and Cholangiocytes and Melatonin Levels in Serum and Bile

We measured the immunoreactivity/expression of AANAT (the rate-limiting enzymes of melatonin biosynthesis)[61] by the following: (1) immunofluorescence in frozen liver sections (6-μm thick) co-stained with CK19 (biliary marker),[45] hepatocyte nuclear factor α (HNF4α),[62] or desmin (marker of HSCs)[63] from mouse and human liver samples; (2) immunohistochemistry in both mouse and human samples; and (3) qPCR in mouse and human cholangiocytes. Furthermore, we performed semiquantification of AANAT IHC with the following formula: positivity area/total area of bile duct) $\times$100 for an image of the portal field by Image-Pro Premier software (Media Cybernetics, Inc, Rockville, MD) on 10 nonoverlapping random fields of 5 mice per group. The bile ducts were selected by their histomorphologic characteristics. Melatonin levels in mouse and human serum and human bile were measured by a commercially available competitive enzyme immunoassay (EIA) kit (LS-F25779; LS-Bio, Seattle, WA).

Evaluation of Organ Histology, Biliary Proliferation, and IBDM

We evaluated the morphology of liver, heart, lung, stomach, pancreas, spleen, kidney, small intestine, and large intestine by H&E staining in paraffin-embedded liver sections (4-μm thick) from the selected groups of mice; slides were evaluated in a blinded fashion by a board-certified pathologist. Biliary proliferation was evaluated by immunohistochemistry for PCNA (marker of cell proliferation)[24] in paraffin-embedded liver sections (4-μm thick) from 4 different mice for each group as well as by qPCR for *PCNA* in isolated cholangiocytes. The stained slides were processed by ImageScope 12.3.3 (Leica Biosystems) to identify PCNA-positive cholangiocytes and analyzed with the following formula: positive-PCNA cell lines/total area $\times$100 for an image of the portal field IBDM was determined by immunohistochemistry for CK19[45] in paraffin-embedded liver sections (4-μm thick); IBDM (DR) was quantified as the area of CK19-positive bile ducts/total area $\times$ 100 for an image of the portal field. The slides were analyzed by Image-Pro Premier

software on 24 nonoverlapping random fields of 5 mice per group.

Evaluation of Biliary Senescence

Biliary senescence was examined by staining for SA-β-GAL by commercially available kits (Millipore Sigma, Billerica, MA) in frozen liver sections (10-μm thick). Observations were made in a blinded fashion with the digital scanner Leica Aperio AT2 (Aperio Scanscope CS System; Aperio Digital Pathology); 20 nonoverlapping random fields were analyzed with the Image-Pro Premier software on 3 mice for each group and quantified as follows: area of SA-β-GAL positivity in biliary duct/total area of biliary $\times$100 for an image of the portal field. Biliary senescence also was evaluated by immunofluorescence for the senescence marker, cyclin-dependent kinase inhibitor 2A (*cdkn2a*/p16), in frozen liver sections (6-μm thick), co-stained with CK19, and immunofluorescent staining was analyzed in a blinded fashion; and qPCR for *cdkn2a* (gene for p16) and *cdkn1a*/cyclin-dependent kinase inhibitor 1A from isolated mouse cholangiocytes.

Evaluation of Liver Fibrosis

Liver fibrosis was assessed by Fast Green/Sirius Red staining in paraffin-embedded liver sections (4-μm thick) in entire sections from 6 different mice for each group by ImageScope version 12.3.3 (Leica Biosystems) using a dedicated algorithm. Liver fibrosis also was evaluated with the following: (1) Masson's Trichrome staining, (2) qPCR for fibrotic genes (*Col1a1* and *Tgfb1*) in total liver samples from 4 mice per group, and (3) TGFβ1 levels in cholangiocyte supernatants by commercially available enzyme-linked immunosorbent assay kits (DY1670-05; R&D Systems, Minneapolis, MN).

Measurement of Biliary Inflammation and Liver Angiogenesis

Liver inflammation was evaluated by semiquantitative immunohistochemistry in paraffin-embedded liver sections (4-μm thick) for F4/80 (a marker of macrophages),[64] for both iNOS and interferon regulatory factor 5, which are M1 macrophage markers involved in promoting inflammation,[65,66] as well as for CD206 (marker of M2 macrophages promoting resolution).[67] Images were quantified with the Image-Pro Premier software on 20 nonoverlapping figures from 5 mice per group and semiquantified as follows: area of F4/80, interferon regulatory factor 5, and CD206 positivity/total area of picture $\times$ 100 for an image of the portal field with Image-Pro Premier software on 20 nonoverlapping random fields of 5 mice per group. Inflammation was assessed further by qPCR for *Il1b* and *Il6* in total liver samples (n = 4 mice for each group) and *Nos2* (gene for iNOS) in the total human liver, as well as isolated mouse cholangiocytes.

Liver angiogenesis was analyzed by the following: (1) immunoreactivity of VEGFA (pro-angiogenic) and (CD31, endothelial cell marker)[4,6] in paraffin-liver sections (4-μm thick) and frozen liver sections (6-μm thick), respectively; (2) mRNA expression of *Vegfc* and *Pecam1* in total liver samples; (3) mRNA expression of *Vegfa*, *Kdr*, and *Flt4* in isolated cholangiocytes; and (4) VEGFA levels in cholangiocyte supernatant by commercially available enzyme-linked immunosorbent assay kit (ab119565; Abcam, Cambridge, MD). VEGFA analysis was performed with the following formula: positivity area (brown)/total area $\times$ 100 for an image of the portal field by ImageScope 12.3.3 (Leica Biosystems).

Measurement of Immunoreactivity/Expression of MT1 in Liver Sections and Cholangiocytes and Expression of pPKA/CREB/Clock Genes/miR200b-3p/Maspin (SERPINB5)/GST Signaling

We previously have shown that short-term melatonin treatment or prolonged dark exposure (that increases melatonin secretion)[5] ameliorates PSC phenotypes in *Mdr2*$^{-/-}$ mice through down-regulation of *miR200b*-dependent angiogenesis.[5] Thus, by Ingenuity Pathway Analysis version 01-16 (Qiagen, Redwood City, CA), we showed a link between the melatonin/MT1 axis and pPKA/CREB/clock genes/*miR200b*/maspin/GST signaling. We first evaluated the hepatic localization/immunoreactivity of MT1 in frozen liver sections (6-μm thick) co-stained with CK19,[45] desmin,[63] or HNF4α[68] from the selected experimental groups; after staining, slides were analyzed as described earlier. Furthermore, we semiquantified the immunoreactivity of MT1 (green) in cholangiocytes (red) with the following formula: MT1 positivity in biliary duct/total area of biliary $\times$100 for an image of the portal field by Image-Pro Premier software on 6 nonoverlapping random fields of 3 mice per group. The mRNA expression of *Mtnr1a* (gene for MT1) also was evaluated by qPCR in isolated mouse cholangiocytes. We measured pPKA substrate by immunohistochemistry in paraffin-embedded liver sections (4-μm thick, co-stained with CK19) as well as the expression of pCREB/CREB in isolated cholangiocytes by immunoblots; as a loading control for protein used for the immunoblots, we used β-actin and Ponceau S staining (total protein loading). The intensity of the bands from immunoblots was analyzed by the Bio-Rad ChemiDoc Imaging System; quantification was expressed as a ratio to total protein loading by ImageJ version 1.52n (National Institutes of Health, Bethesda, MD) because of the dynamic changes in the mouse model of liver fibrosis.[69,70]

The immunoreactivity and mRNA/protein expression of selected clock genes (*Per1*, *Cry1, Clock*, and *Arntl*) was evaluated by immunofluorescence in frozen mouse liver sections (6-μm thick) and by qPCR in isolated mouse cholangiocytes. Furthermore, we co-stained clock genes (*Per1*, *Cry1, Clock*, and *Arntl*) with CK19 in normal controls and PSC samples and semiquantified the biliary immunoreactivity as follows: clock gene positivity in biliary duct/total area of biliary $\times$ 100 for an image of the portal field by Image-Pro Premier software on 3 nonoverlapping random fields of 3 human samples per group. We measured the mRNA expression of *miR200b* and *Serpinb*5 (gene for maspin) in isolated cholangiocytes by qPCR, and the antioxidant activity of GST with commercially available GST assay kits

(CS0410; Sigma-Aldrich) in isolated cholangiocytes. In normal control and PSC late-stage patients, we measured the following: (1) the mRNA expression of *miR200b*/*Serpinb5* in total liver samples by qPCR; (2) GST activity by commercially available GST assay kits; and (3) protein expression of maspin in total liver samples; as loading control for the amount of protein used for the immunoblots, we used glyceraldehyde-3-phosphate dehydrogenase. The quantification was expressed as a ratio to glyceraldehyde-3-phosphate dehydrogenase by ImageJ version 1.52n.

In Vitro Effect of Melatonin on Cholangiocyte Phenotypes

The in vitro studies were performed in P92 cells (PSC cholangiocyte cell line immortalized with SV40) isolated from liver explant tissue from a 60-year-old man who was a late-stage PSC patient obtained through Dr Ekser under an approved protocol (see later). The explant liver tissue was cut into small pieces using sterile scissors and washed in 1× phosphate-buffered saline, and then incubated in Dulbecco's modified Eagle medium–F12 (Lonza, Walkersville, MD) solution containing 1.66 mg/mL of collagenase type XI and 10% antibiotic-antimycotic, for 30 minutes in a shaking water bath at 37°C. The digested liver tissue was filtered through a sterilized gauze first and then a 100-μm cell strainer. To remove hepatocytes, the lysate was centrifuged at 100 × *g* for 4 minutes at 4ºC, and the pellet was discarded. Next, we centrifuged the supernatant at 700 × *g* for 5 minutes to collect nonparenchymal cells (NPCs) washed in Dulbecco's modified Eagle medium–F12 containing 10% antibiotic-antimycotic before centrifuging again at 700 × *g* for 5 minutes. The NPC was resuspended in H69 media,[3] plated on collagen-coated flasks (BD Biosciences, San Jose, CA), and allowed to grow to confluence. At the second passage, the NPC was sorted via fluorescence-activated cell sorting with an Epithelial cell adhesion molecule (EpCAM) antibody (surface epithelial marker expressed by cholangiocytes, EA125/anti-EP-CAM; Progen, Wayne, PA).[71] EpCAM-positive cholangiocytes[72] (33.1%) (Figure 14*A*) were immortalized by transfection SV40 antigen into cells using a lentiviral system (G203; Applied Biological Materials, Inc, Richmond, British Columbia, Canada) and cultured them to expand the population. The purity of the PSC line was characterized phenotypically in cell smears by immunofluorescence for CK19 co-stained with HNF4α (a marker of hepatocytes),[62] desmin (a marker of HSCs),[63] CD68 (a marker of macrophages), or CD31 (a marker of endothelial cells).[4,73] Next, PSC cell lines after serum starvation for 24 hours were treated with 0.46% of ethanol (vehicle) or 10^{-3} mol/L melatonin[29] dissolved in 0.46% of ethanol for 24 hours before measuring the mRNA expression of proliferation (*PCNA*, *MKI67*), senescence (*CDKN1A*, *CDKN2A*), fibrosis (*FN1*, *TGFB1*, and *ACTA2*), and angiogenesis (*VEGFA*) markers, as well as *MTNR1A*, clock genes, and *miR-200b* by qPCR. Finally, PSC cell lines (2×10^{10}) treated with vehicle/melatonin were plated on collagen-coated chambers (BD Biosciences) for immunostaining analysis for clock genes and MT1 receptor co-stained with CK19.

Animal Models

Animal experiments were performed with protocols approved by the Indiana University School of Medicine Institutional Animal Care and Use Committee. The studies were performed in 12-week-old (20–25 g) male FVB/NJ (Friend Virus B NIH Jackson) WT and *Mdr2*$^{-/-}$ mice treated with vehicle or melatonin for 12 weeks. All mice were killed at 24 weeks of age. FVB/NJ WT mice were purchased from Jackson Laboratory (Bar Harbor, ME); *Mdr2*$^{-/-}$ mice are available in our breeding colony. All mice had access to drinking water with/without melatonin (1.03 mg melatonin intake per mouse per day) for 12 weeks ad libitum; melatonin was dissolved in 1 L water (0.03% melatonin), and water intake was measured every 3 days during treatment (Figure 1*A*). All mice were housed in a temperature-controlled environment (20°C–22°C) with 12:12 light/dark cycles, and had access to standard chow ad libitum. Mice were injected with euthasol, 50 mg/kg body weight, before collecting serum, bile, tissue/organs, and cholangiocytes. Liver and body weight were recorded from the selected groups of animals (Table 1).

Cholangiocyte Isolation and Human Samples

Cholangiocytes were purified by immunoaffinity separation using a monoclonal antibody (IgG2a, a gift from Dr R. Faris, Brown University, Providence, RI) against an antigen expressed by all intrahepatic cholangiocytes.[74] Liver tissues from healthy patients (n = 2) and late-stage male PSC patients (n = 10) were obtained from Dr Burcin Ekser under a protocol approved by the Indiana University School of Medicine Indianapolis Institutional Review Board. Liver specimens from late-stage PSC were obtained from the explant during liver transplantation, and each patient provided written informed consent to participate in the study. Additional control liver samples (n = 4) derived from healthy patients with no history of chronic liver diseases were purchased from Sekisui XenoTech (Kansas City, KS). The human control and late-stage PSC patient information are shown in Table 4.

All authors had access to the study data, and reviewed and approved the final manuscript.

Statistical Analysis

GraphPad Prism 8.3.1 software (San Diego, CA) was used to perform the statistical analyses. Data are expressed as the means ± SEM. Differences between groups were evaluated by the Student unpaired *t* test when 2 groups were analyzed or by 1-way analysis of variance when more than 2 groups were analyzed followed by an appropriate post hoc test. A *P* value less than .05 was considered statistically significant.

References

1. Karlsen TH, Folseraas T, Thorburn D, Vesterhus M. Primary sclerosing cholangitis - a comprehensive review. J Hepatol 2017;67:1298–1323.
2. Pollheimer MJ, Trauner M, Fickert P. Will we ever model PSC? - "it's hard to be a PSC model". Clin Res Hepatol Gastroenterol 2011;35:792–804.

3. Tabibian JH, O'Hara SP, Splinter PL, Trussoni CE, LaRusso NF. Cholangiocyte senescence by way of N-ras activation is a characteristic of primary sclerosing cholangitis. Hepatology 2014;59:2263–2275.
4. Kennedy L, Francis H, Invernizzi P, Venter J, Wu N, Carbone M, Gershwin ME, Bernuzzi F, Franchitto A, Alvaro D, Marzioni M, Onori P, Gaudio E, Sybenga A, Fabris L, Meng F, Glaser S, Alpini G. Secretin/secretin receptor signaling mediates biliary damage and liver fibrosis in early-stage primary biliary cholangitis. FASEB J 2019;33:10269–10279.
5. Wu N, Meng F, Zhou T, Han Y, Kennedy L, Venter J, Francis H, DeMorrow S, Onori P, Invernizzi P, Bernuzzi F, Mancinelli R, Gaudio E, Franchitto A, Glaser S, Alpini G. Prolonged darkness reduces liver fibrosis in a mouse model of primary sclerosing cholangitis by miR-200b down-regulation. FASEB J 2017;31:4305–4324.
6. Zhou T, Wu N, Meng F, Venter J, Giang TK, Francis H, Kyritsi K, Wu C, Franchitto A, Alvaro D, Marzioni M, Onori P, Mancinelli R, Gaudio E, Glaser S, Alpini G. Knockout of secretin receptor reduces biliary damage and liver fibrosis in Mdr2($^{-/-}$) mice by diminishing senescence of cholangiocytes. Lab Invest 2018;98:1449–1464.
7. Coon SL, Mazuruk K, Bernard M, Roseboom PH, Klein DC, Rodriguez IR. The human serotonin N-acetyltransferase (EC 2.3.1.87) gene (AANAT): structure, chromosomal localization, and tissue expression. Genomics 1996;34:76–84.
8. Renzi A, Glaser S, DeMorrow S, Mancinelli R, Meng F, Franchitto A, Venter J, White M, Francis H, Han Y, Alvaro D, Gaudio E, Carpino G, Ueno Y, Onori P, Alpini G. Melatonin inhibits cholangiocyte hyperplasia in cholestatic rats by interaction with MT1 but not MT2 melatonin receptors. Am J Physiol Gastrointest Liver Physiol 2011;301:G634–G643.
9. Hu C, Zhao L, Tao J, Li L. Protective role of melatonin in early-stage and end-stage liver cirrhosis. J Cell Mol Med 2019;23:7151–7162.
10. Baiocchi L, Zhou T, Liangpunsakul S, Ilaria L, Milana M, Meng F, Kennedy L, Kusumanchi P, Yang Z, Ceci L, Glaser S, Francis H, Alpini G. Possible application of melatonin treatment in human diseases of the biliary tract. Am J Physiol Gastrointest Liver Physiol 2019;317:G651–G660.
11. Ostrycharz E, Wasik U, Kempinska-Podhorodecka A, Banales JM, Milkiewicz P, Milkiewicz M. Melatonin protects cholangiocytes from oxidative stress-induced proapoptotic and proinflammatory stimuli via miR-132 and miR-34. Int J Mol Sci 2020;21:9667.
12. Renzi A, DeMorrow S, Onori P, Carpino G, Mancinelli R, Meng F, Venter J, White M, Franchitto A, Francis H, Han Y, Ueno Y, Dusio G, Jensen KJ, Greene JJ Jr, Glaser S, Gaudio E, Alpini G. Modulation of the biliary expression of arylalkylamine N-acetyltransferase alters the autocrine proliferative responses of cholangiocytes in rats. Hepatology 2013;57:1130–1141.
13. Chen L, Zhou T, Wu N, O'Brien A, Venter J, Ceci L, Kyritsi K, Onori P, Gaudio E, Sybenga A, Xie L, Wu C, Fabris L, Invernizzi P, Zawieja D, Liangpunsakul S, Meng F, Francis H, Alpini G, Huang Q, Glaser S. Pinealectomy or light exposure exacerbates biliary damage and liver fibrosis in cholestatic rats through decreased melatonin synthesis. Biochim Biophys Acta Mol Basis Dis 2019;1865:1525–1539.
14. Wu N, Carpino G, Ceci L, Baiocchi L, Francis H, Kennedy L, Zhou T, Chen L, Sato K, Kyritsi K, Meadows V, Ekser B, Franchitto A, Mancinelli R, Onori P, Gaudio E, Glaser S, Alpini G. Melatonin receptor 1A, but not 1B, knockout decreases biliary damage and liver fibrosis during cholestatic liver injury. Hepatology 2022;75:797–813.
15. Gaudio E, Onori P, Pannarale L, Alvaro D. Hepatic microcirculation and peribiliary plexus in experimental biliary cirrhosis: a morphological study. Gastroenterology 1996;111:1118–1124.
16. Chen L, Wu N, Kennedy L, Francis H, Ceci L, Zhou T, Samala N, Kyritsi K, Wu C, Sybenga A, Ekser B, Dar W, Atkins C, Meadows V, Glaser S, Alpini G. Inhibition of secretin/secretin receptor axis ameliorates NAFLD phenotypes. Hepatology 2021;74:1845–1863.
17. Govaere O, Cockell S, Van Haele M, Wouters J, Van Delm W, Van den Eynde K, Bianchi A, van Eijsden R, Van Steenbergen W, Monbaliu D, Nevens F, Roskams T. High-throughput sequencing identifies aetiology-dependent differences in ductular reaction in human chronic liver disease. J Pathol 2019;248:66–76.
18. Lahiri DK, Ge YW, Sharman EH, Bondy SC. Age-related changes in serum melatonin in mice: higher levels of combined melatonin and 6-hydroxymelatonin sulfate in the cerebral cortex than serum, heart, liver and kidney tissues. J Pineal Res 2004;36:217–223.
19. Alpini G, Lenzi R, Sarkozi L, Tavoloni N. Biliary physiology in rats with bile ductular cell hyperplasia. Evidence for a secretory function of proliferated bile ductules. J Clin Invest 1988;81:569–578.
20. Guicciardi ME, Trussoni CE, Krishnan A, Bronk SF, Lorenzo Pisarello MJ, O'Hara SP, Splinter PL, Gao Y, Vig P, Revzin A, LaRusso NF, Gores GJ. Macrophages contribute to the pathogenesis of sclerosing cholangitis in mice. J Hepatol 2018;69:676–686.
21. Sharma JN, Al-Omran A, Parvathy SS. Role of nitric oxide in inflammatory diseases. Inflammopharmacology 2007;15:252–259.
22. Yi WJ, Kim TS. Melatonin protects mice against stress-induced inflammation through enhancement of M2 macrophage polarization. Int Immunopharmacol 2017;48:146–158.
23. Carbajo-Pescador S, Ordonez R, Benet M, Jover R, Garcia-Palomo A, Mauriz JL, Gonzalez-Gallego J. Inhibition of VEGF expression through blockade of Hif1alpha and STAT3 signalling mediates the anti-angiogenic effect of melatonin in HepG2 liver cancer cells. Br J Cancer 2013;109:83–91.
24. Gaudio E, Barbaro B, Alvaro D, Glaser S, Francis H, Ueno Y, Meininger CJ, Franchitto A, Onori P, Marzioni M, Taffetani S, Fava G, Stoica G, Venter J, Reichenbach R, De Morrow S, Summers R, Alpini G. Vascular endothelial growth factor stimulates rat cholangiocyte proliferation

via an autocrine mechanism. Gastroenterology 2006; 130:1270–1282.
25. Alvaro D, Onori P, Metalli VD, Svegliati-Baroni G, Folli F, Franchitto A, Alpini G, Mancino MG, Attili AF, Gaudio E. Intracellular pathways mediating estrogen-induced cholangiocyte proliferation in the rat. Hepatology 2002; 36:297–304.
26. Yin S, Li X, Meng Y, Finley RL Jr, Sakr W, Yang H, Reddy N, Sheng S. Tumor-suppressive maspin regulates cell response to oxidative stress by direct interaction with glutathione S-transferase. J Biol Chem 2005; 280:34985–34996.
27. von Gall C, Schneider-Huther I, Pfeffer M, Dehghani F, Korf HW, Stehle JH. Clock gene protein mPER1 is rhythmically synthesized and under cAMP control in the mouse pineal organ. J Neuroendocrinol 2001; 13:313–316.
28. Han Y, DeMorrow S, Invernizzi P, Jing Q, Glaser S, Renzi A, Meng F, Venter J, Bernuzzi F, White M, Francis H, Lleo A, Marzioni M, Onori P, Alvaro D, Torzilli G, Gaudio E, Alpini G. Melatonin exerts by an autocrine loop antiproliferative effects in cholangiocarcinoma: its synthesis is reduced favoring cholangiocarcinoma growth. Am J Physiol Gastrointest Liver Physiol 2011;301:G623–G633.
29. Osseni RA, Rat P, Bogdan A, Warnet JM, Touitou Y. Evidence of prooxidant and antioxidant action of melatonin on human liver cell line HepG2. Life Sci 2000; 68:387–399.
30. Hwang SJ, Jung Y, Song YS, Park S, Park Y, Lee HJ. Enhanced anti-angiogenic activity of novel melatonin-like agents. J Pineal Res 2021;71:e12739.
31. Wu N, Baiocchi L, Zhou T, Kennedy L, Ceci L, Meng F, Sato K, Wu C, Ekser B, Kyritsi K, Kundu D, Chen L, Meadows V, Franchitto A, Alvaro D, Onori P, Gaudio E, Lenci I, Francis H, Glaser S, Alpini G. Functional role of the secretin/secretin receptor signaling during cholestatic liver injury. Hepatology 2020;72:2219–2227.
32. Andersen LP, Gogenur I, Rosenberg J, Reiter RJ. The safety of melatonin in humans. Clin Drug Investig 2016; 36:169–175.
33. Gonciarz M, Gonciarz Z, Bielanski W, Mularczyk A, Konturek PC, Brzozowski T, Konturek SJ. The pilot study of 3-month course of melatonin treatment of patients with nonalcoholic steatohepatitis: effect on plasma levels of liver enzymes, lipids and melatonin. J Physiol Pharmacol 2010;61:705–710.
34. Ferlazzo N, Andolina G, Cannata A, Costanzo MG, Rizzo V, Curro M, Ientile R, Caccamo D. Is melatonin the cornucopia of the 21st century? Antioxidants (Basel) 2020;9:1088.
35. Sato K, Meng F, Francis H, Wu N, Chen L, Kennedy L, Zhou T, Franchitto A, Onori P, Gaudio E, Glaser S, Alpini G. Melatonin and circadian rhythms in liver diseases: functional roles and potential therapies. J Pineal Res 2020;68:e12639.
36. Dubocovich ML, Yun K, Al-Ghoul WM, Benloucif S, Masana MI. Selective MT2 melatonin receptor antagonists block melatonin-mediated phase advances of circadian rhythms. FASEB J 1998;12:1211–1220.
37. Dubocovich ML, Masana MI, Iacob S, Sauri DM. Melatonin receptor antagonists that differentiate between the human Mel1a and Mel1b recombinant subtypes are used to assess the pharmacological profile of the rabbit retina ML1 presynaptic heteroreceptor. Naunyn Schmiedebergs Arch Pharmacol 1997;355:365–375.
38. Roseboom PH, Coon SL, Baler R, McCune SK, Weller JL, Klein DC. Melatonin synthesis: analysis of the more than 150-fold nocturnal increase in serotonin N-acetyltransferase messenger ribonucleic acid in the rat pineal gland. Endocrinology 1996;137:3033–3045.
39. Christ E, Pfeffer M, Korf HW, von Gall C. Pineal melatonin synthesis is altered in period 1 deficient mice. Neuroscience 2010;171:398–406.
40. Klein DC. Arylalkylamine N-acetyltransferase: "the Timezyme". J Biol Chem 2007;282:4233–4237.
41. Rui BB, Chen H, Jang L, Li Z, Yang JM, Xu WP, Wei W. Melatonin upregulates the activity of AMPK and attenuates lipid accumulation in alcohol-induced rats. Alcohol Alcohol 2016;51:11–19.
42. Wang J, Zhuo Z, Ma X, Liu Y, Xu J, He C, Fu Y, Wang F, Ji P, Zhang L, Liu G. Melatonin alleviates the suppressive effect of hypoxanthine on oocyte nuclear maturation and restores meiosis via the melatonin receptor 1 (MT1)-mediated pathway. Front Cell Dev Biol 2021;9:648148.
43. Muhlbauer E, Albrecht E, Bazwinsky-Wutschke I, Peschke E. Melatonin influences insulin secretion primarily via MT(1) receptors in rat insulinoma cells (INS-1) and mouse pancreatic islets. J Pineal Res 2012; 52:446–459.
44. Baiocchi L, Lenci I, Milana M, Kennedy L, Sato K, Zhang W, Ekser B, Ceci L, Meadows V, Glaser S, Alpini G, Francis H. Cyclic AMP signaling in biliary proliferation: a possible target for cholangiocarcinoma treatment? Cells 2021;10:1692.
45. Glaser S, Meng F, Han Y, Onori P, Chow BK, Francis H, Venter J, McDaniel K, Marzioni M, Invernizzi P, Ueno Y, Lai JM, Huang L, Standeford H, Alvaro D, Gaudio E, Franchitto A, Alpini G. Secretin stimulates biliary cell proliferation by regulating expression of microRNA 125b and microRNA let7a in mice. Gastroenterology 2014; 146:1795–1808 e12.
46. Wu N, Meng F, Invernizzi P, Bernuzzi F, Venter J, Standeford H, Onori P, Marzioni M, Alvaro D, Franchitto A, Gaudio E, Glaser S, Alpini G. The secretin/secretin receptor axis modulates liver fibrosis through changes in transforming growth factor-beta1 biliary secretion in mice. Hepatology 2016;64:865–879.
47. Han K, Zhang Y, Yang Z. Cilostazol protects rats against alcohol-induced hepatic fibrosis via suppression of TGF-beta1/CTGF activation and the cAMP/Epac1 pathway. Exp Ther Med 2019;17:2381–2388.
48. Osawa Y, Oboki K, Imamura J, Kojika E, Hayashi Y, Hishima T, Saibara T, Shibasaki F, Kohara M, Kimura K. Inhibition of cyclic adenosine monophosphate (cAMP)-response element-binding protein (CREB)-binding protein (CBP)/beta-catenin reduces liver fibrosis in mice. EBioMedicine 2015;2:1751–1758.
49. Taysi S, Koc M, Buyukokuroglu ME, Altinkaynak K, Sahin YN. Melatonin reduces lipid peroxidation and nitric

oxide during irradiation-induced oxidative injury in the rat liver. J Pineal Res 2003;34:173–177.
50. Shearn CT, Orlicky DJ, Petersen DR. Dysregulation of antioxidant responses in patients diagnosed with concomitant primary sclerosing cholangitis/inflammatory bowel disease. Exp Mol Pathol 2018;104:1–8.
51. Mariotti V, Fiorotto R, Cadamuro M, Fabris L, Strazzabosco M. New insights on the role of vascular endothelial growth factor in biliary pathophysiology. JHEP Rep 2021;3:100251.
52. Maass N, Nagasaki K, Ziebart M, Mundhenke C, Jonat W. Expression and regulation of tumor suppressor gene maspin in breast cancer. Clin Breast Cancer 2002; 3:281–287.
53. Cher ML, Biliran HR Jr, Bhagat S, Meng Y, Che M, Lockett J, Abrams J, Fridman R, Zachareas M, Sheng S. Maspin expression inhibits osteolysis, tumor growth, and angiogenesis in a model of prostate cancer bone metastasis. Proc Natl Acad Sci U S A 2003; 100:7847–7852.
54. Kim KJ, Choi JS, Kang I, Kim KW, Jeong CH, Jeong JW. Melatonin suppresses tumor progression by reducing angiogenesis stimulated by HIF-1 in a mouse tumor model. J Pineal Res 2013;54:264–270.
55. Lissoni P, Rovelli F, Malugani F, Bucovec R, Conti A, Maestroni GJ. Anti-angiogenic activity of melatonin in advanced cancer patients. Neuro Endocrinol Lett 2001; 22:45–47.
56. Montagnese S, Nsemi LM, Cazzagon N, Facchini S, Costa L, Bergasa NV, Amodio P, Floreani A. Sleep-wake profiles in patients with primary biliary cirrhosis. Liver Int 2013;33:203–209.
57. Crespo I, Fernandez-Palanca P, San-Miguel B, Alvarez M, Gonzalez-Gallego J, Tunon MJ. Melatonin modulates mitophagy, innate immunity and circadian clocks in a model of viral-induced fulminant hepatic failure. J Cell Mol Med 2020;24:7625–7636.
58. He C, Shen W, Chen C, Wang Q, Lu Q, Shao W, Jiang Z, Hu H. Circadian rhythm disruption influenced hepatic lipid metabolism, gut microbiota and promoted cholesterol gallstone formation in mice. Front Endocrinol (Lausanne) 2021;12:723918.
59. Forsyth CB, Voigt RM, Burgess HJ, Swanson GR, Keshavarzian A. Circadian rhythms, alcohol and gut interactions. Alcohol 2015;49:389–398.
60. Jensen LD, Cao Z, Nakamura M, Yang Y, Brautigam L, Andersson P, Zhang Y, Wahlberg E, Lanne T, Hosaka K, Cao Y. Opposing effects of circadian clock genes bmal1 and period 2 in regulation of VEGF-dependent angiogenesis in developing zebrafish. Cell Rep 2012; 2:231–241.
61. Klein DC, Coon SL, Roseboom PH, Weller JL, Bernard M, Gastel JA, Zatz M, Iuvone PM, Rodriguez IR, Begay V, Falcon J, Cahill GM, Cassone VM, Baler R. The melatonin rhythm-generating enzyme: molecular regulation of serotonin N-acetyltransferase in the pineal gland. Recent Prog Horm Res 1997;52:307–357; discussion 57–58.
62. Zhou T, Kyritsi K, Wu N, Francis H, Yang Z, Chen L, O'Brien A, Kennedy L, Ceci L, Meadows V, Kusumanchi P, Wu C, Baiocchi L, Skill NJ, Saxena R, Sybenga A, Xie L, Liangpunsakul S, Meng F, Alpini G, Glaser S. Knockdown of vimentin reduces mesenchymal phenotype of cholangiocytes in the Mdr2(-/-) mouse model of primary sclerosing cholangitis (PSC). EBioMedicine 2019;48:130–142.
63. Yokoi Y, Namihisa T, Kuroda H, Komatsu I, Miyazaki A, Watanabe S, Usui K. Immunocytochemical detection of desmin in fat-storing cells (Ito cells). Hepatology 1984; 4:709–714.
64. Kennedy L, Meadows V, Demieville J, Hargrove L, Virani S, Glaser S, Zhou T, Rinehart E, Jaeger V, Kyritsi K, Pham L, Alpini G, Francis H. Biliary damage and liver fibrosis are ameliorated in a novel mouse model lacking l-histidine decarboxylase/histamine signaling. Lab Invest 2020;100:837–848.
65. Xiong H, Zhu C, Li F, Hegazi R, He K, Babyatsky M, Bauer AJ, Plevy SE. Inhibition of interleukin-12 p40 transcription and NF-kappaB activation by nitric oxide in murine macrophages and dendritic cells. J Biol Chem 2004;279:10776–10783.
66. Krausgruber T, Blazek K, Smallie T, Alzabin S, Lockstone H, Sahgal N, Hussell T, Feldmann M, Udalova IA. IRF5 promotes inflammatory macrophage polarization and TH1-TH17 responses. Nat Immunol 2011;12:231–238.
67. Bertani FR, Mozetic P, Fioramonti M, Iuliani M, Ribelli G, Pantano F, Santini D, Tonini G, Trombetta M, Businaro L, Selci S, Rainer A. Classification of M1/M2-polarized human macrophages by label-free hyperspectral reflectance confocal microscopy and multivariate analysis. Sci Rep 2017;7:8965.
68. Bonzo JA, Ferry CH, Matsubara T, Kim JH, Gonzalez FJ. Suppression of hepatocyte proliferation by hepatocyte nuclear factor 4alpha in adult mice. J Biol Chem 2012; 287:7345–7356.
69. Zhang B, Wu X, Liu J, Song L, Song Q, Wang L, Yuan D, Wu Z. beta-Actin: not a suitable internal control of hepatic fibrosis caused by Schistosoma japonicum. Front Microbiol 2019;10:66.
70. Ceci L, Francis H, Zhou T, Giang T, Yang Z, Meng F, Wu N, Kennedy L, Kyritsi K, Meadows V, Wu C, Liangpunsakul S, Franchitto A, Sybenga A, Ekser B, Mancinelli R, Onori P, Gaudio E, Glaser S, Alpini G. Knockout of the tachykinin receptor 1 in the Mdr2(-/-) (Abcb4(-/-)) mouse model of primary sclerosing cholangitis reduces biliary damage and liver fibrosis. Am J Pathol 2020;190:2251–2266.
71. Lanzoni G, Cardinale V, Carpino G. The hepatic, biliary, and pancreatic network of stem/progenitor cell niches in humans: a new reference frame for disease and regeneration. Hepatology 2016;64:277–286.
72. Betjes MG, Haks MC, Tuk CW, Beelen RH. Monoclonal antibody EBM11 (anti-CD68) discriminates between dendritic cells and macrophages after short-term culture. Immunobiology 1991;183:79–87.
73. Breiteneder-Geleff S, Soleiman A, Kowalski H, Horvat R, Amann G, Kriehuber E, Diem K, Weninger W, Tschachler E, Alitalo K, Kerjaschki D. Angiosarcomas express mixed endothelial phenotypes of blood and

lymphatic capillaries: podoplanin as a specific marker for lymphatic endothelium. Am J Pathol 1999;154:385–394.
74. Ishii M, Vroman B, LaRusso NF. Isolation and morphologic characterization of bile duct epithelial cells from normal rat liver. Gastroenterology 1989;97:1236–1247.

Received April 11, 2022. Accepted July 11, 2022.

Correspondence
Address correspondence to: Shannon Glaser, PhD, Department of Medical Physiology, Texas A&M University College of Medicine, MREBII–Office 2342, 8447 Riverside Parkway, Bryan, Texas 77807. e-mail: sglaser@tamu.edu.

CRediT Authorship Contributions
Shannon Glaser, PhD (Conceptualization: Supporting; Formal analysis: Supporting; Funding acquisition: Equal; Methodology: Supporting; Resources: Equal; Supervision: Supporting; Validation: Supporting; Writing – original draft: Supporting; Writing – review & editing: Supporting)
Ludovica Ceci (Conceptualization: Lead; Data curation: Lead; Formal analysis: Equal; Methodology: Equal; Project administration: Equal; Supervision: Equal; Writing – original draft: Equal; Writing – review & editing: Equal)
Lixian Chen (Data curation: Supporting; Formal analysis: Supporting; Investigation: Supporting; Software: Supporting; Writing – review & editing: Supporting)
Leonardo Baiocchi (Writing – original draft: Equal; Writing – review & editing: Equal)
Nan Wu (Data curation: Supporting; Investigation: Supporting; Writing – review & editing: Supporting)
Lindsey Kennedy (Conceptualization: Supporting; Funding acquisition: Supporting; Methodology: Supporting; Writing – review & editing: Supporting)
Guido Carpino (Data curation: Supporting; Investigation: Supporting; Writing – review & editing: Supporting)
Konstantina Kyritsi (Data curation: Supporting; Investigation: Supporting; Writing – review & editing: Supporting)
Travis Owen (Data curation: Supporting; Investigation: Supporting)
Debjyoti Kundu (Writing – review & editing: Supporting)
Tianhao Zhou (Data curation: Supporting; Investigation: Supporting; Writing – review & editing: Supporting)
Amelia Sybenga (Data curation: Supporting; Investigation: Supporting)
Abdulkadir Isidan (Data curation: Supporting; Investigation: Supporting; Writing – review & editing: Supporting)
Burcin Ekser (Writing – review & editing: Supporting)
Antonio Franchitto (Writing – review & editing: Supporting)
Paolo Onori (Writing – review & editing: Supporting)
Eugenio Gaudio (Writing – review & editing: Supporting)
Romina Mancinelli (Data curation: Supporting; Investigation: Supporting)
Heather Francis (Funding acquisition: Supporting; Resources: Supporting; Writing – review & editing: Supporting)
Gianfranco Alpini (Conceptualization: Supporting; Data curation: Supporting; Funding acquisition: Equal; Methodology: Supporting; Resources: Equal; Supervision: Supporting; Visualization: Supporting; Writing – original draft: Supporting; Writing – review & editing: Supporting)

Conflicts of interest
The authors disclose no conflicts.

Funding
This work was supported by the Hickam Endowed Chair, Gastroenterology, Medicine, Indiana University, the Indiana University Health–Indiana University School of Medicine Strategic Research Initiative, a Senior Research Career Scientist Award (IK6 BX004601), VA Merit award 5I01BX000574 (G.A.), Research Career Scientist Award IK6BX005226 and VA Merit award 1I01BX003031 (H.F.), Career Development Award-2 1IK2BX005306 from the US Department of Veteran's Affairs, Biomedical Laboratory Research and Development Service (L.K.), National Institutes of Health grants DK108959 and DK119421 (H.F.), grants DK054811, DK115184, DK076898, DK107310, DK110035, DK062975, AA025997, and AA025157 (G.A. and S.G.), and PSC Partners Seeking a Cure (G.A.). This material is the result of work supported by resources at Indiana University and the Richard L. Roudebush VA Medical Center, Indianapolis, IN, and Medical Physiology, Medical Research Building, Temple, TX. The views expressed in this article are those of the authors and do not necessarily represent the views of the Department of Veterans Affairs.